Electronic Supplementary Material (ESI) for Polymer Chemistry.

Ring Opening Polymerization and Copolymerization for Polyester and Polycarbonate Formation by a Diamino-bis(phenolate) Chromium(III) Catalyst

*Cyler W. Vos, James Beament, and Christopher M. Kozak**

Department of Chemistry, Memorial University of Newfoundland and Labrador, St. John's, Newfoundland, Canada A1C 5S7.

* Author to whom correspondence should be addressed. E-mail: ckozak@mun.ca

Supplementary Information

Table of Contents:

Instrumentation

Polymer molar masses and dispersities were determined by gel permeation chromatography (GPC) using an Agilent 1260 Infinity high-performance liquid chromatograph coupled to a Wyatt Technologies triple detector system (light scattering, viscometer, and refractive index) and equipped with one Phenogel 10^3 Å, 300 mm × 4.60 mm column and one 10^4 Å, 300 mm × 4.60 mm column (covering mass ranges of 1000 − 75 000 and 5000 − 500 000 g mol^{-1}, respectively). HPLC grade THF was used as the eluent at a flow rate of 0.3 mL min^{-1} at 25 °C. Processing of the GPC data were done using the Astra 6 software package. Ring opening polymerization and copolymerization reactions using in situ FTIR spectroscopy were performed using a 100 mL stainless steel Parr 4560 reactor with motorized mechanical stirrer and heating mantle. The reactor was modified to be equipped with a Mettler Toledo SiComp ATR Sentinel sensor connected to a ReactIR 15 base unit using a silver-halide Fiber-to-Sentinel conduit.

^{1}H NMR spectra were recorded on Bruker AVANCE III 300 MHz and AVANCE 500 MHz spectrometers with chemical shifts in parts per million (ppm) relative to the residual proton signals in solvent ($CDCl_3$). The ^{1}H diffusion ordered spectroscopy (DOSY) NMR spectra of the purified polymers were recorded using a Bruker AVANCE 500 MHz spectrometer. ^{1}H{^{1}H} NMR spectra for polymer stereochemistry studies were performed on a Bruker AVANCE II 600 MHz spectrometer. Deuterated solvents were purchased from Cambridge Isotope Laboratories Inc. and used without further purification.

MALDI-TOF mass spectrometry on the polymers was performed using a Bruker ultrafleXtreme MALDI TOF/TOF analyzer with a Bruker smartbeam-II laser (up to 2 kHz, operating at 355 nm) for linear and reflectron mode. Mass spectra of 1000 shots were accumulated. 2,5-Dihydroxybenzoic acid (DHB) was used as the matrix for polymer analysis where it was dissolved in THF at a concentration of 15 mg mL^{-1}. The characterization of **2** by MALDI-TOF MS was done previously using anthracene as a matrix. Repeated analysis for this work gave identical results.[35] A cationizing agent salt solution (sodium trifluoroacetate, NaTFA) in THF was used at a concentration of 1 mol L^{-1}. Polymer was dissolved in THF to a concentration of 10 mg mL^{-1}, then combined with the DHBA matrix and NaTFA in a ratio of 3:20:1 µL, respectively. Aliquots of 0.5 µL of these solutions were spotted and the solvent was allowed to evaporate. MALDI-TOF MS data were processed, and images prepared using MestReNova software with the mass analysis plug-in.

^{1}H NMR Spectra of epoxide-initiated ROP and ROCOP using 2

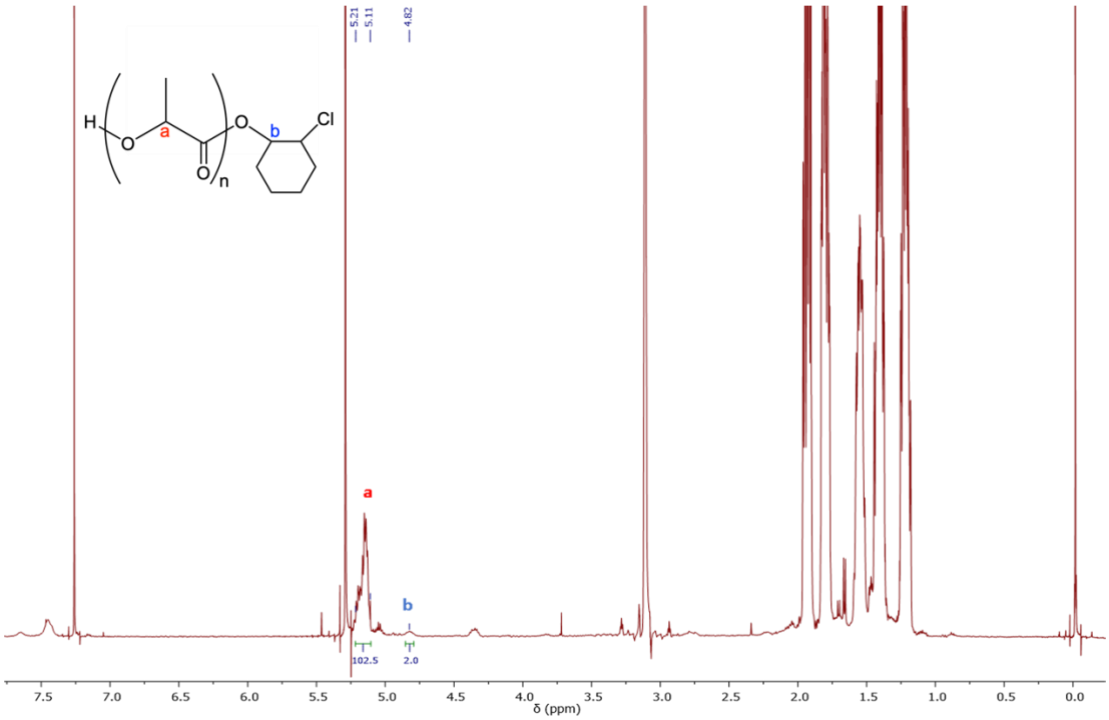

Figure S1. Crude ^{1}H NMR (300 MHz, $CDCl_3$) spectrum of ROP of *rac*-LA using **2** as initiator and CHO as solvent and co-initiator, $[rac\text{-LA}]_0$:$[CHO]_0$:$[\mathbf{2}]_0$ = 100:500:1, 80 °C, 2 h (Table 1, entry 8). Conversion is taken from integration of the methine region of the polymer and the monomer. polyester repeat units are monitored from resonances in the range of 5.11 – 5.21 ppm. CHO end groups are identified from resonance corresponding to OCH_2 signal at 4.82 ppm. No PCHO ether units are seen indicative by no obvious resonance between 3.30 – 3.65 ppm.

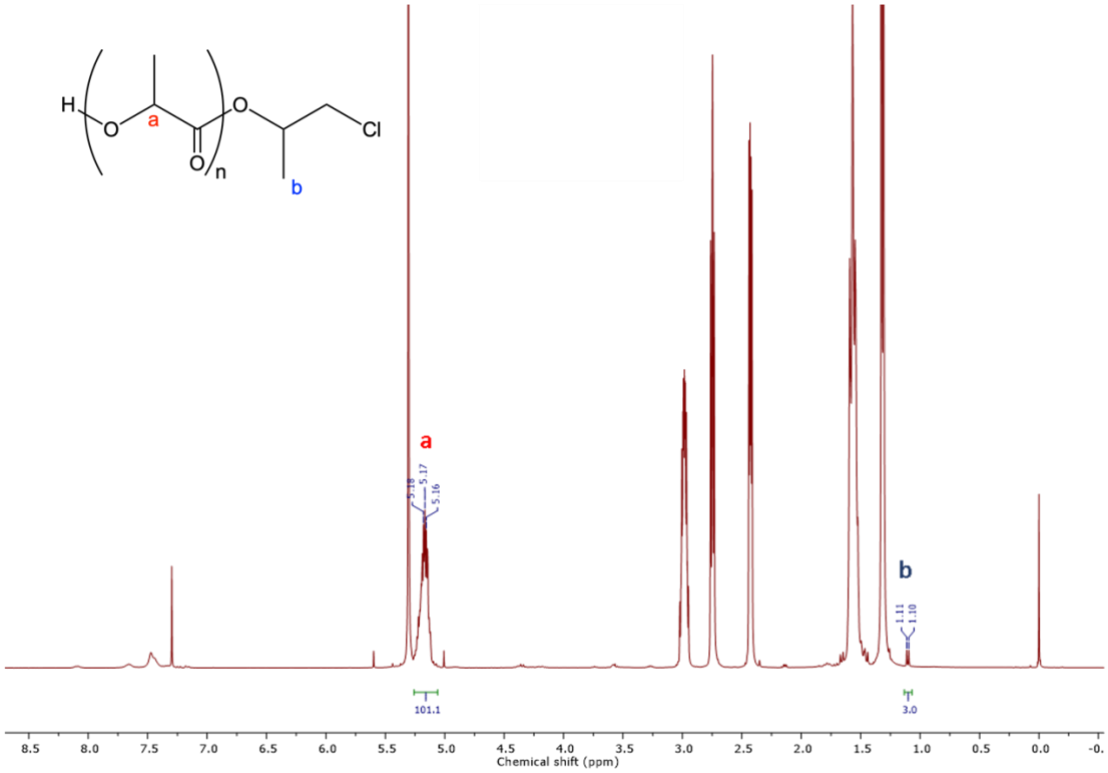

Figure S2. Crude ^{1}H NMR (300 MHz, $CDCl_3$) spectrum of ROP of *rac*-LA using **2** as initiator and PO as solvent and co-initiator, [*rac*-LA]$_0$:[PO]$_0$:[**2**]$_0$ = 100:500:1, 40 °C, 1 h (Table 1, entry 10). Conversion is taken from integration of the methine region of the polymer and the monomer. PO end groups are identified from a doublet at 1.1 ppm.

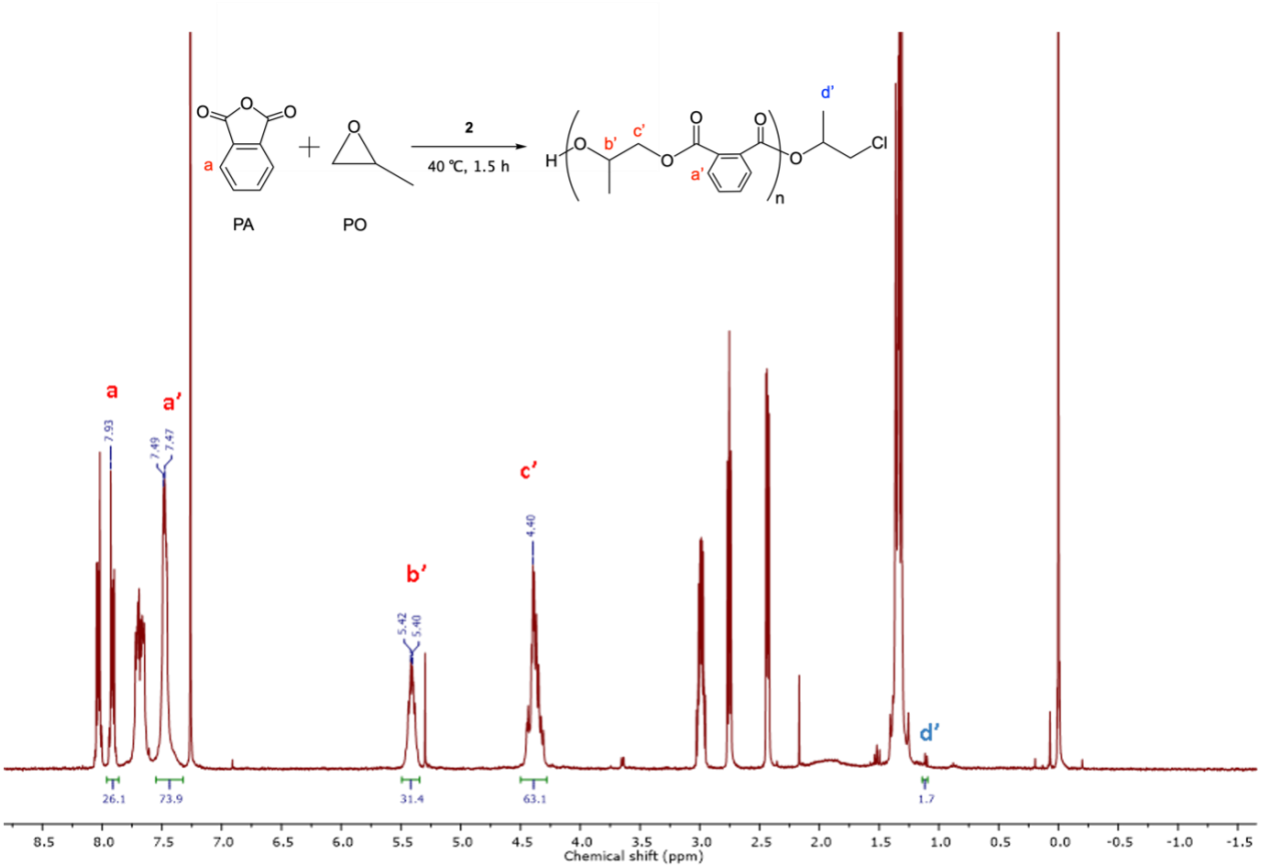

Figure S3. Crude ^{1}H NMR (300 MHz, $CDCl_3$) spectrum of ROCOP of PA using **2** as initiator and PO as reactant and co-initiator, $[PA]_0$:$[PO]_0$:$[\mathbf{2}]_0$ = 100:500:1, 40 °C, 1.5 h (Table 2, entry 5). Conversion is taken from integration of the aromatic region of PA from the polymer (7.46 – 7.50 ppm) and the monomer (7.85 – 7.94 ppm). PPO production is monitored from resonances in the range of 3.5 – 3.7 ppm. PO end groups are identified from a doublet at 1.1 ppm.

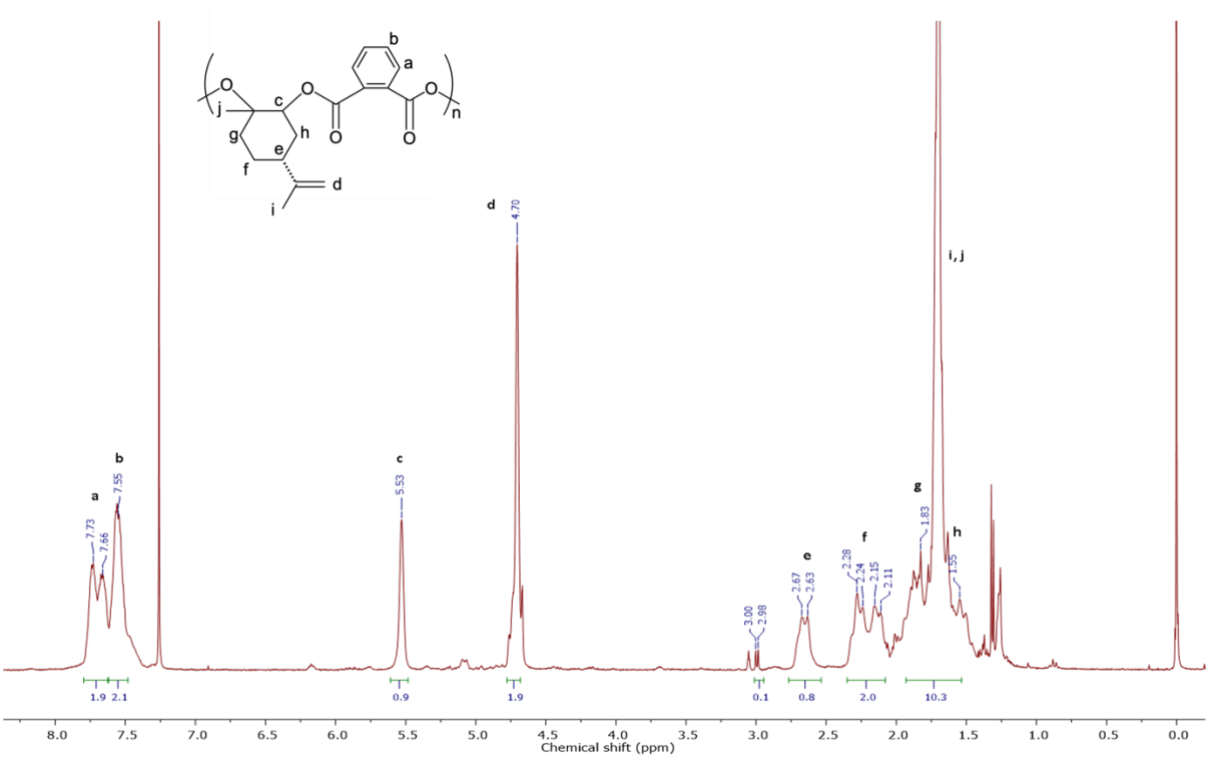

Figure S4. ^{1}H NMR spectrum (300 MHz, $CDCl_3$) of ROCOP of PA and LO using **2** as initiator, $[PA]_0$:$[LO]_0$:$[\mathbf{2}]_0$ = 100:500:1, 130 °C, 1 h (Table 2, entry 6). Conversion is taken from integration of the aromatic region of the polymer (7.37 – 7.78 ppm) and the monomer (7.85 – 7.94 ppm). Ether linkages are monitored using resonances at 3.5 – 3.7 ppm. LO end groups are identified from a doublet at 1.1 ppm.

Kinetic studies of ROP and ROCOP reactions using CHO and 2

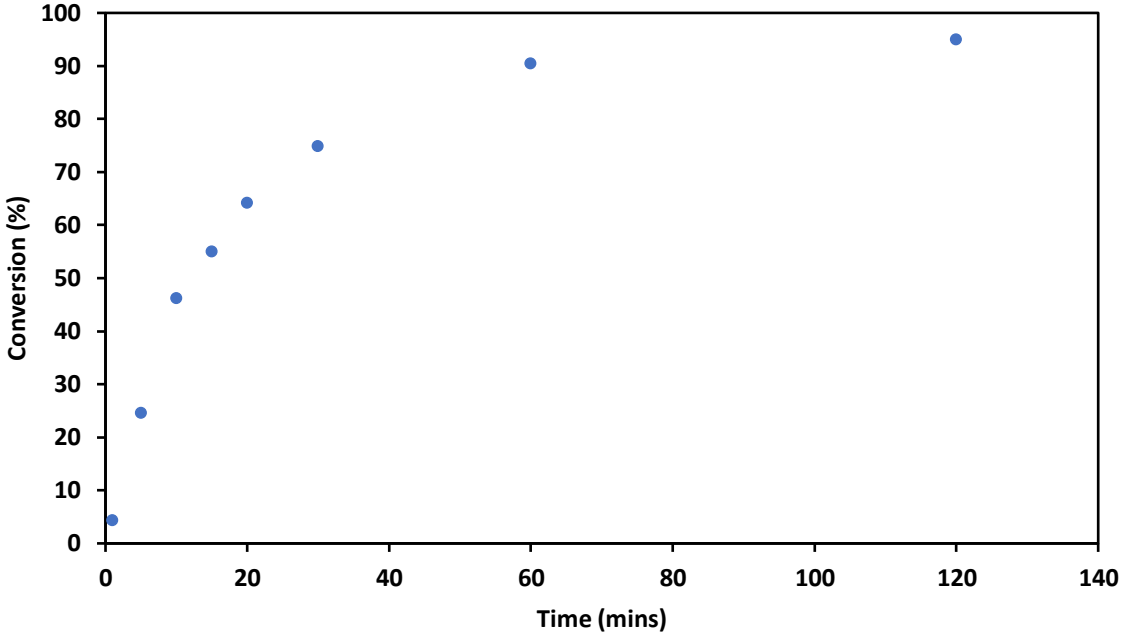

Figure S5. Conversion vs time for the aliquots monitored ROP of *rac*-LA using **2** as initiator and CHO as solvent and co-initiator, [*rac*-LA]$_0$:[CHO]$_0$:[**2**]$_0$ = 100:500:1, 80 °C (Table 1, entry 5). Conversion is taken from integration of the methine region of the PLA and the monomer.

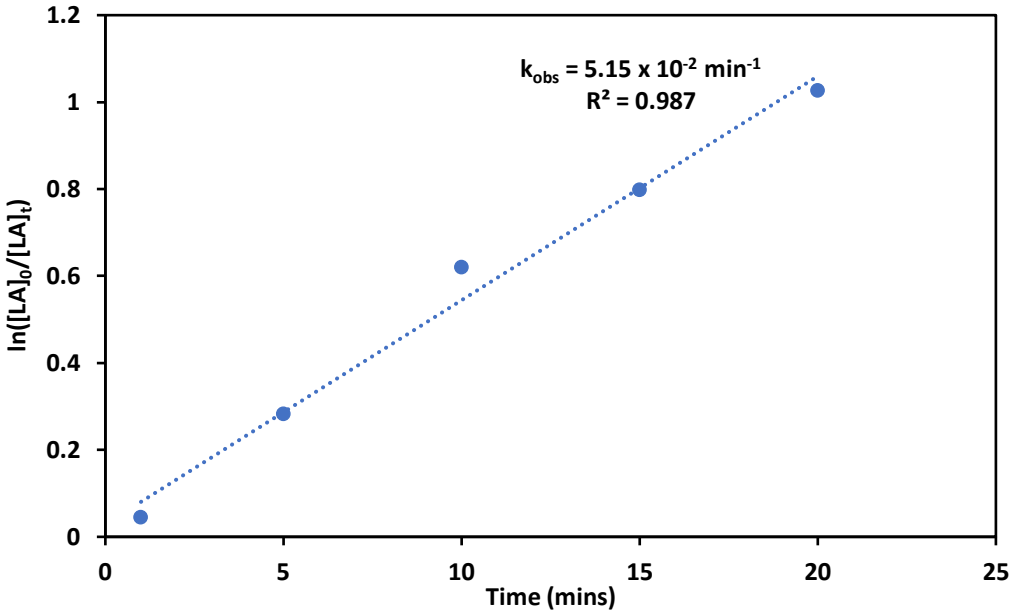

Figure S6. Linearized plot for the ROP of *rac*-LA using **2** as initiator and CHO as solvent and co-initiator, [*rac*-LA]$_0$:[CHO]$_0$:[**2**]$_0$ = 100:500:1, 80 °C (Table 1, entry 5). Conversion is taken from integration of the methine region of PLA and the monomer.

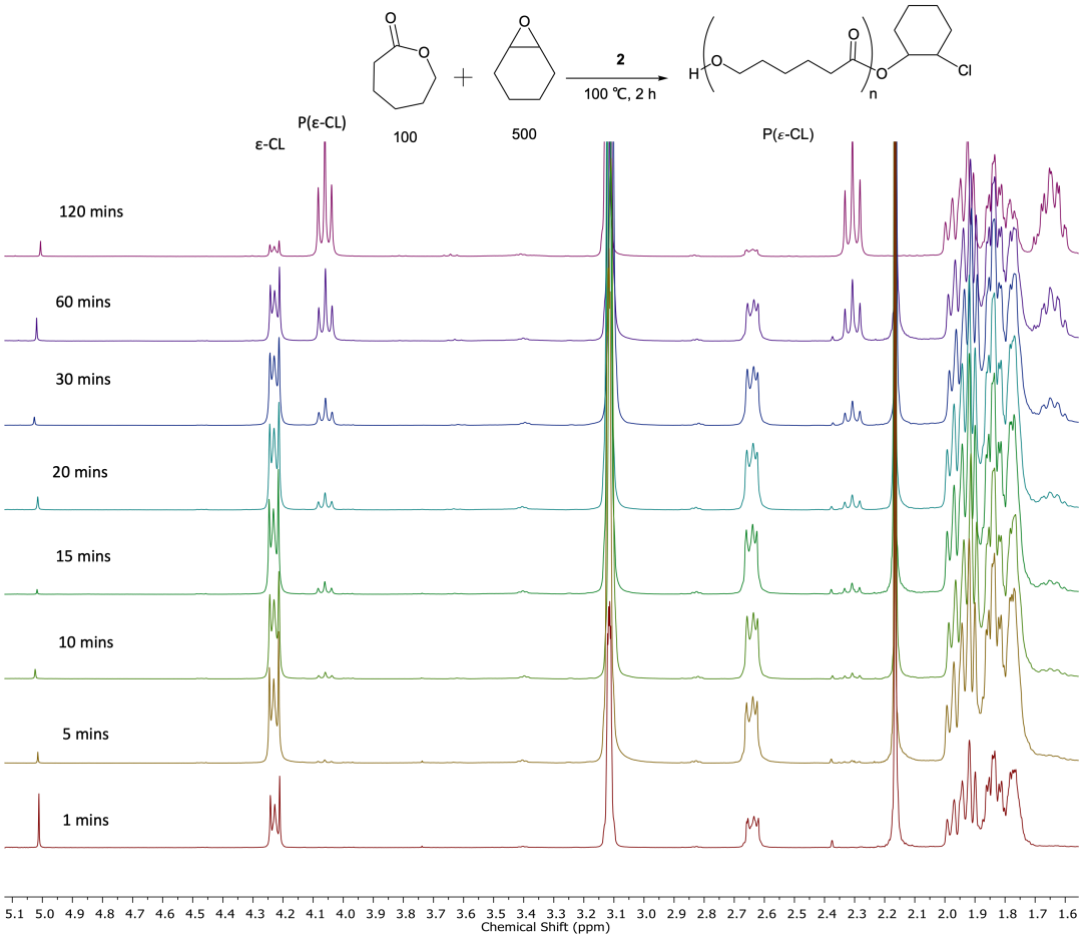

Figure S7. Stacked ^{1}H NMR (300 MHz, $CDCl_3$) spectra of aliquots from ROP of ε-CL using **2** as initiator and CHO as solvent and co-initiator. Conditions as in Table 1, entry 9, $[\varepsilon\text{-CL}]_0$:$[CHO]_0$:$[\mathbf{2}]_0$ = 100:500:1, 100 °C. Conversion is taken from integration of the polymer (4.05 – 4.10 ppm) and monomer (4.20 – 4.60 ppm) regions.

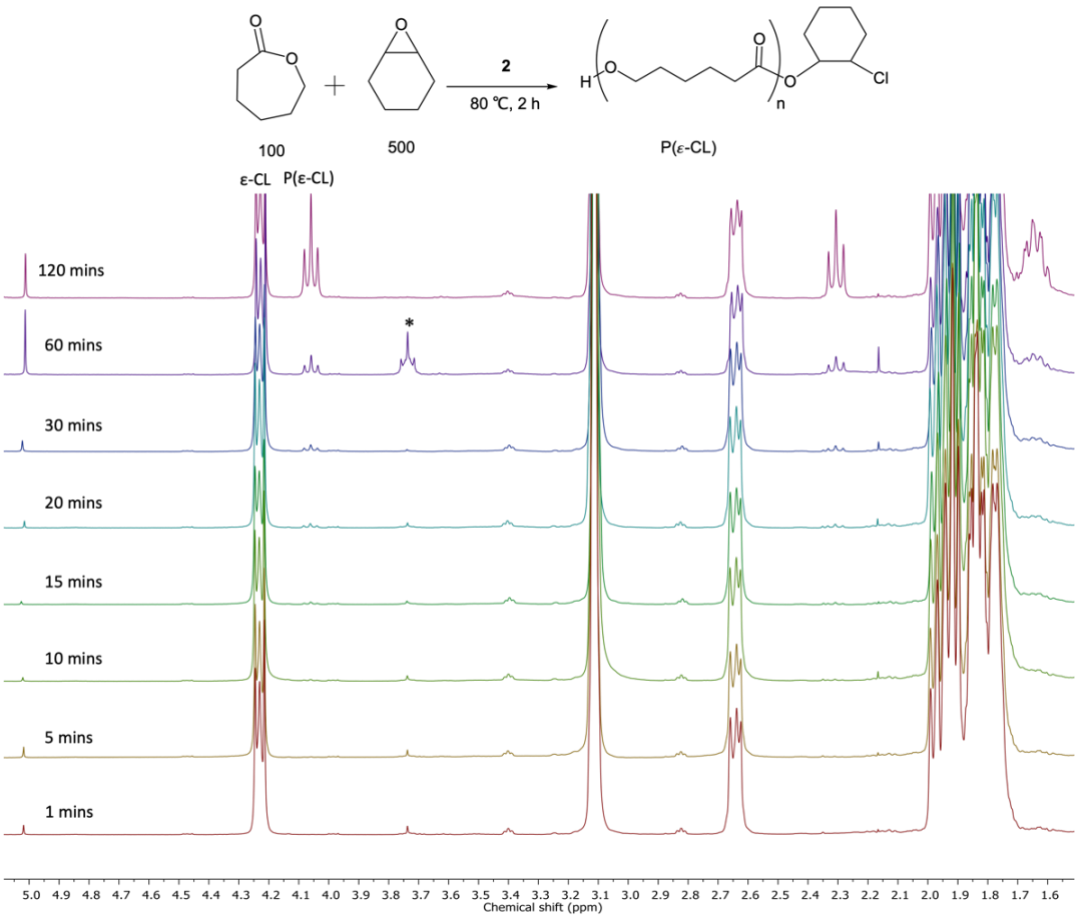

Figure S8. Stacked ^{1}H NMR (300 MHz, $CDCl_3$) spectra of the aliquots monitored ROP of ε-CL using **2** as initiator and CHO as solvent and co-initiator, $[\varepsilon\text{-CL}]_0$:$[CHO]_0$:$[\mathbf{2}]_0$ = 100:500:1, 80 °C (Table 1, entry 8). Conversion is taken from integration of the P(ε-CL) region (4.05 – 4.10 ppm) and the monomer (4.20 – 4.60 ppm). *During 60 min aliquot ^{1}H NMR spectrum, THF contaminant.

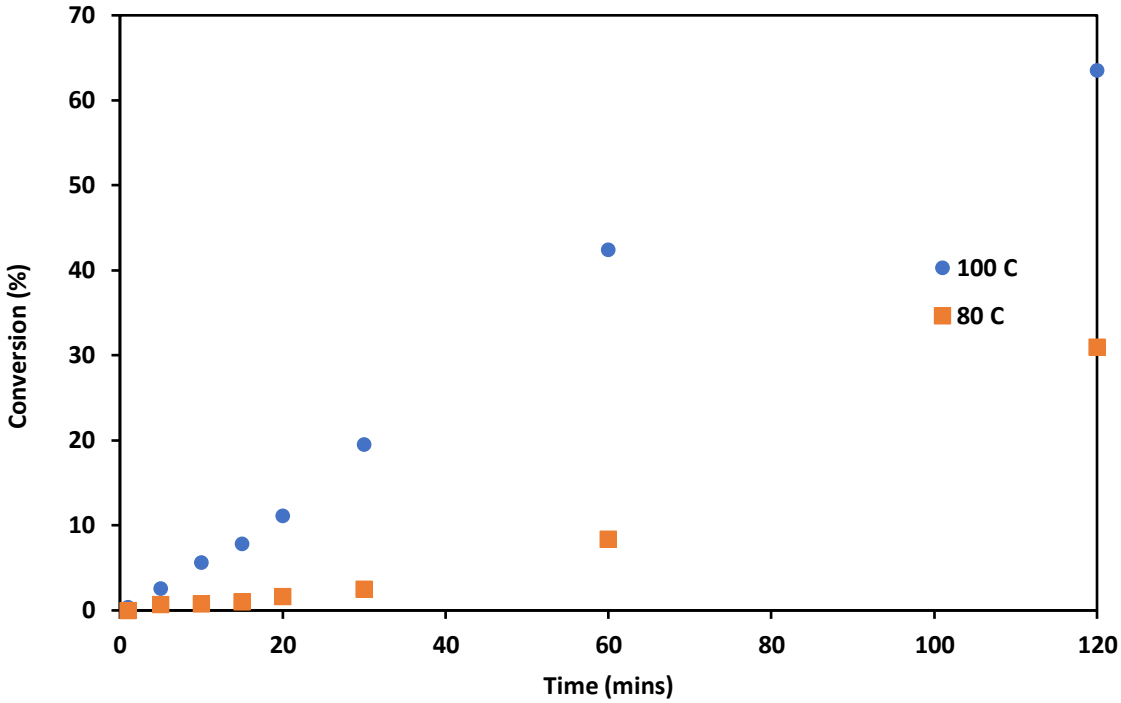

Figure S9. Conversion vs time for the aliquots monitored ROP of ε-CL using **2** as initiator and CHO as solvent and co-initiator, $[\varepsilon\text{-CL}]_0:[\text{CHO}]_0:[\mathbf{2}]_0 = 100:500:1$ (Table 1, entries 8 and 9), ▪ = 80 °C,.• = 100 °C. Conversion is taken from integration of the methine region of P(ε-CL) and the monomer.

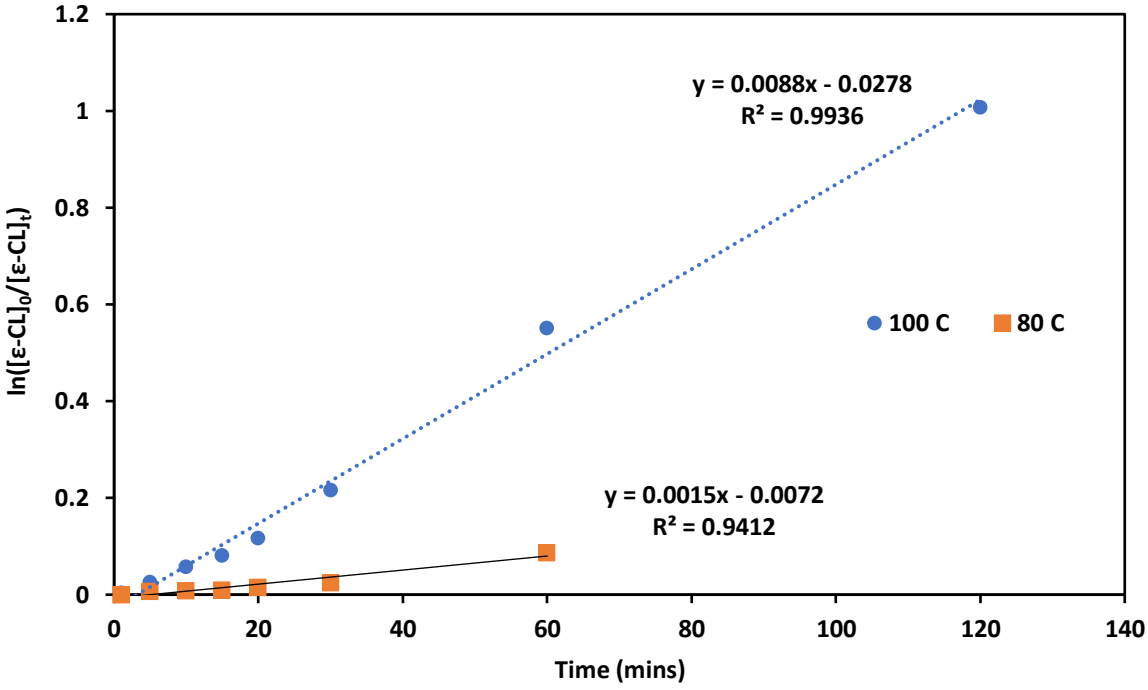

Figure S10. First-order plot of the ROP of ε-CL using **2** as initiator and CHO as solvent and co-initiator $[\varepsilon\text{-CL}]_0:[\text{CHO}]_0:[\mathbf{2}]_0 = 100:500:1$ (Table 1, entries 8 and 9), ▪ = 80 °C,.• = 100 °C. Conversion is taken from integration of the methine region of the polymer and the monomer. Line of each series represents best fit.

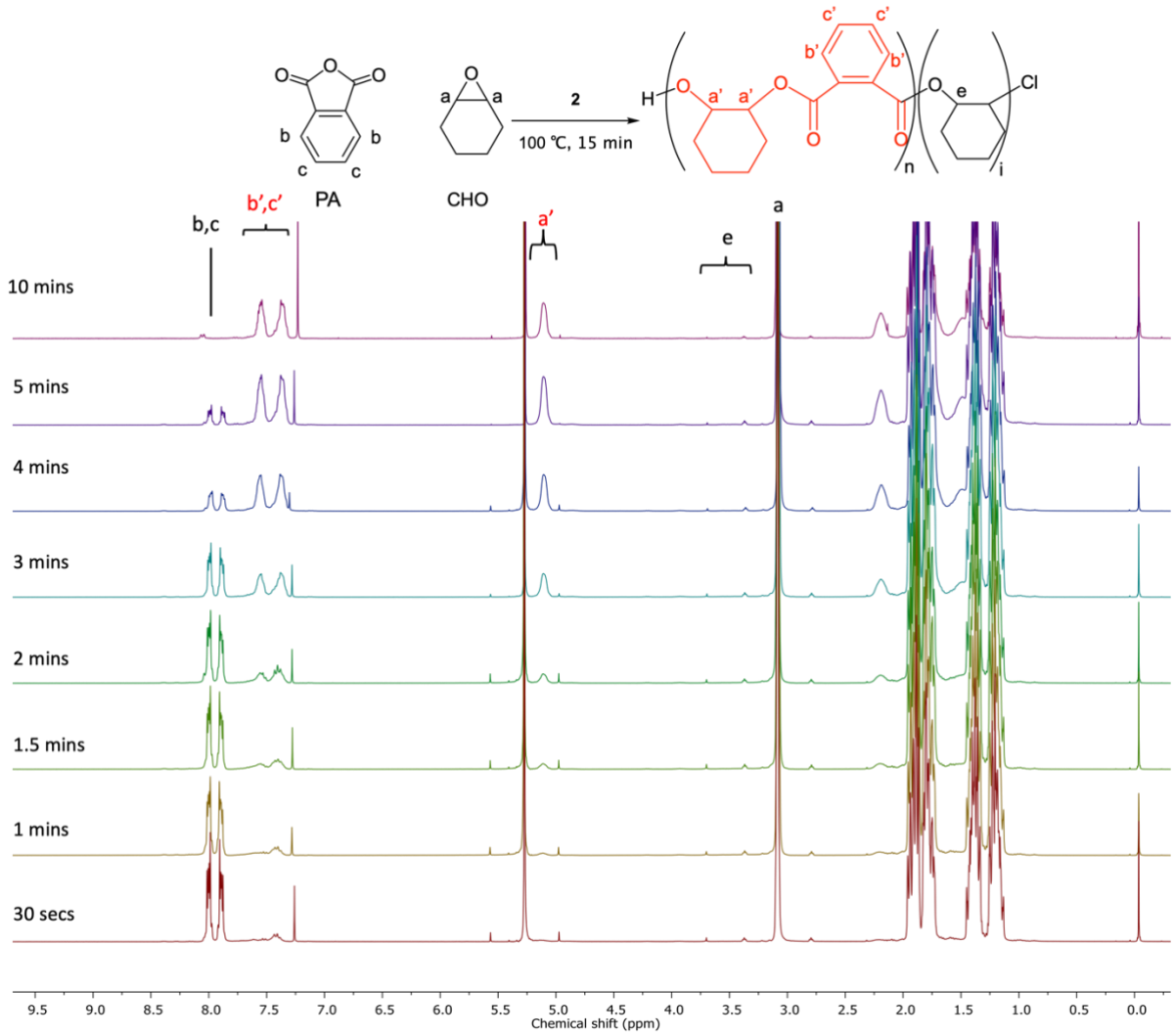

Figure S11. Stacked ^{1}H NMR (300 MHz, $CDCl_3$) spectra of the aliquots monitored ROCOP of PA and CHO using **2** as initiator and CHO as solvent and reagent, $[PA]_0$:$[CHO]_0$:$[\mathbf{2}]_0$ = 100:500:1, 100 °C (Table 2, entry 3). Conversion is taken from integration of the aromatic region of PA in the polymer (7.35 – 7.60 ppm) and the monomer (7.84 – 8.04 ppm).

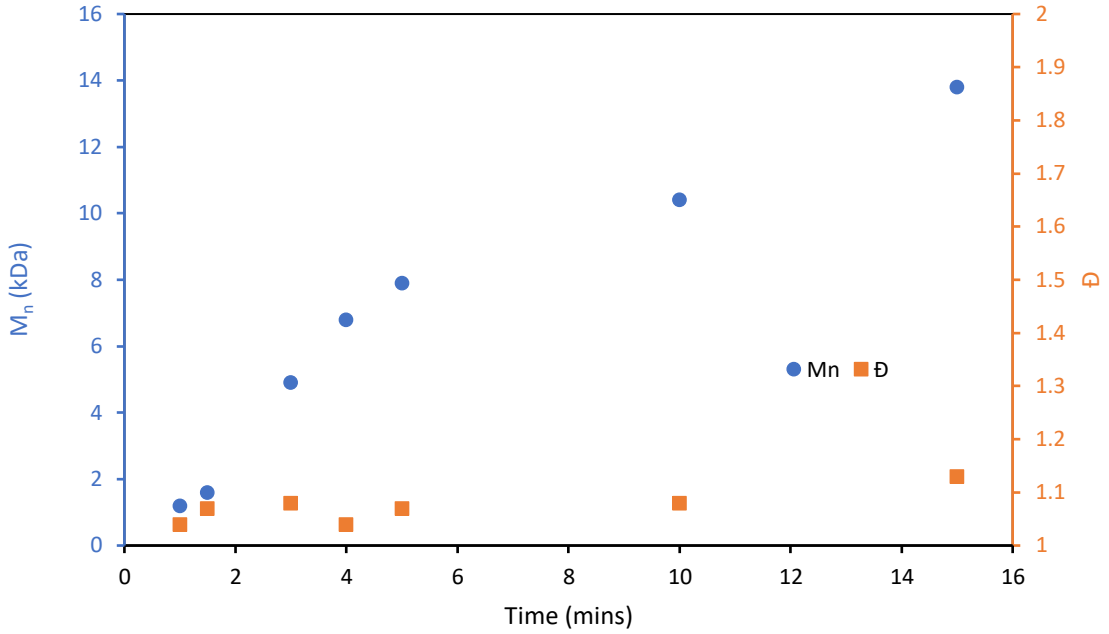

Figure S12. M_n^{GPC} and $Đ$ over time for the ROCOP of PA and CHO using **2** as initiator and CHO as solvent and reagent $[PA]_0:[CHO]_0:[\mathbf{2}]_0$ = 100:500:1, 100 °C (Table 2, entry 3) M_n^{GPC} and $Đ$ are calculated from GPC in THF using triple detection methods.

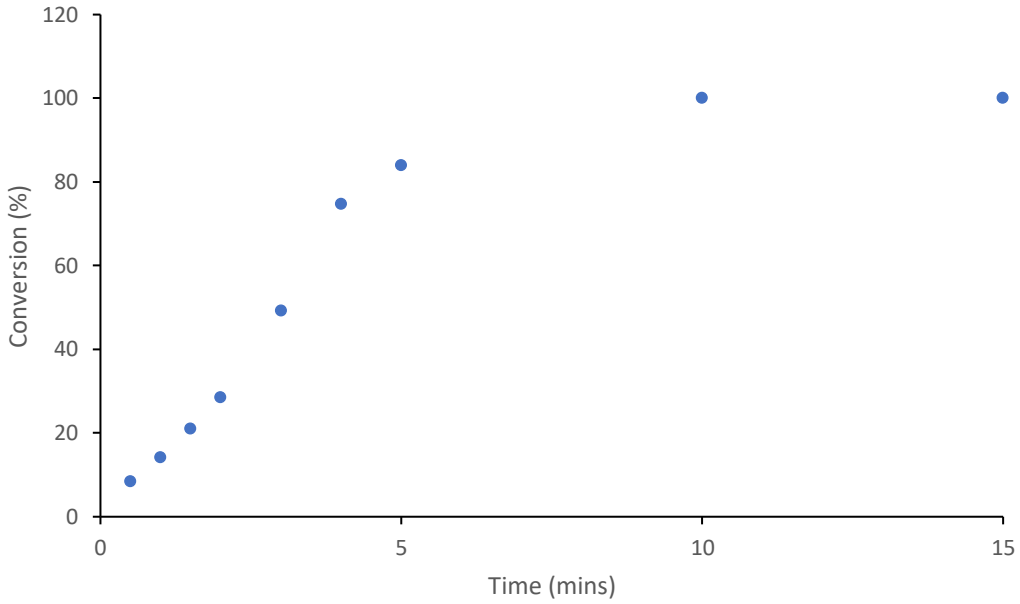

Figure S13. Conversion of PA vs time for ROCOP of CHO and PA using **2** as initiator done neat in CHO using $[PA]_0:[CHO]_0:[\mathbf{2}]_0$ = 100:500:1, 100 °C (Table 2, entry 3). PA conversion to polyester is taken from integration of the methine region of the polymer and the monomer.

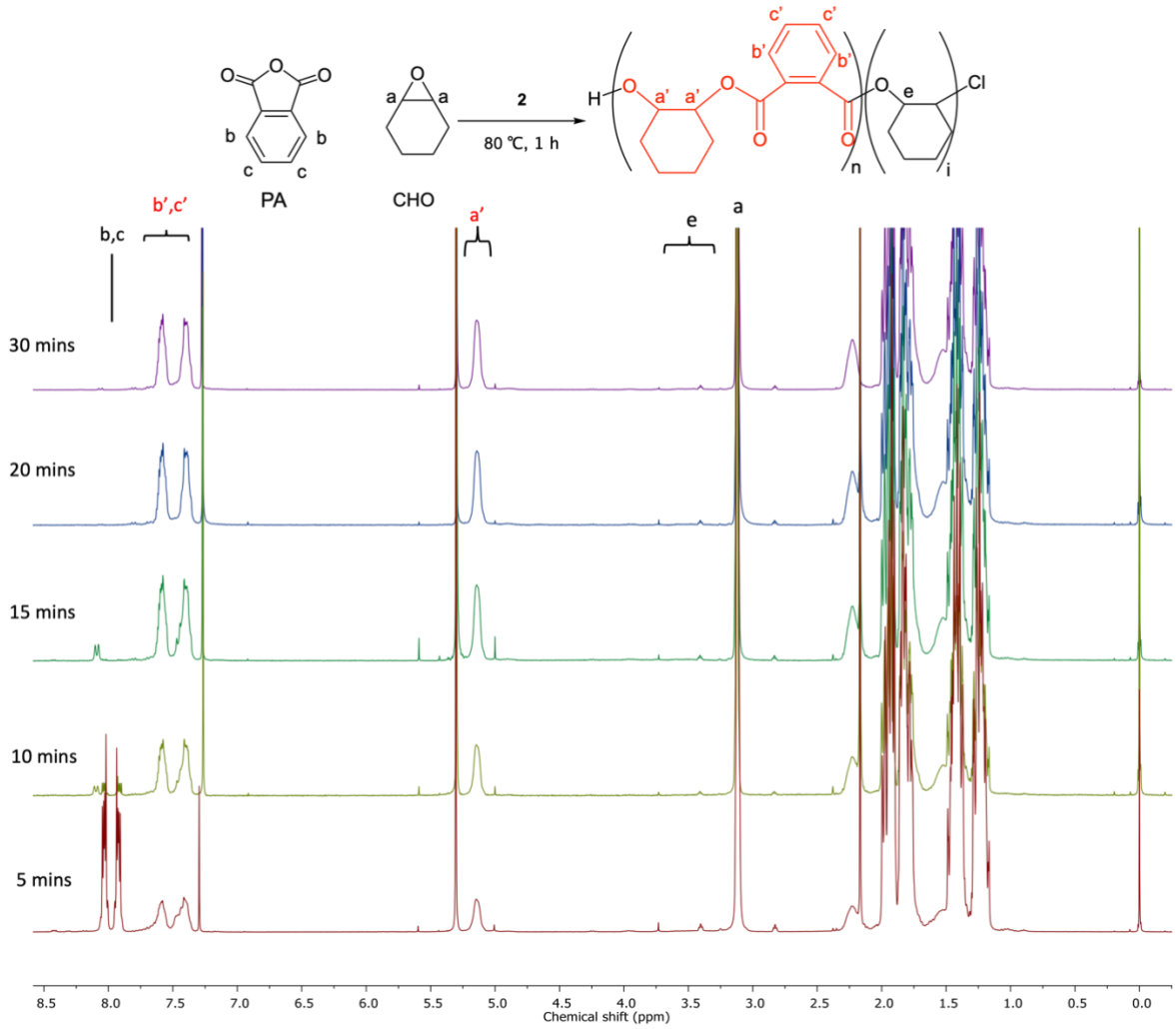

Figure S14. Stacked ^{1}H NMR (300 MHz, $CDCl_3$) spectra of the aliquots monitored ROCOP of PA and CHO using **2** as initiator and CHO as solvent and reagent $[PA]_0$:$[CHO]_0$:$[\mathbf{2}]_0$ = 100:500:1, 80 °C (Table 2, entry 4). Conversion is taken from integration of the aromatic region of PA in the polymer (7.35 – 7.60 ppm) and the monomer (7.84 – 8.04 ppm). Aliquots stopped at 30 minutes as full conversion of PA to polyester was observed after 20 min.

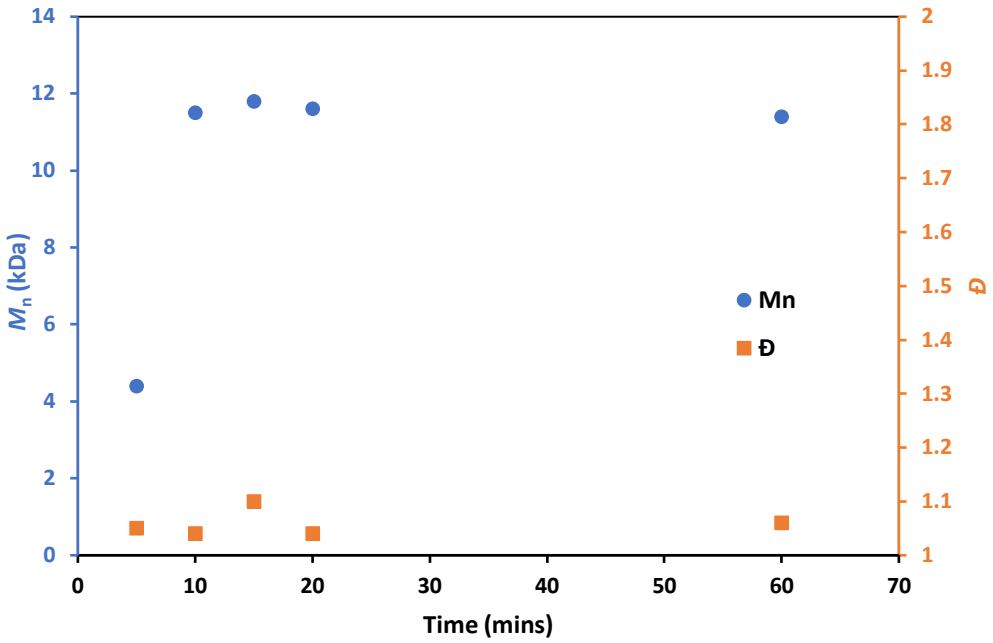

Figure S15. M_n^{GPC} and $Đ$ over time for the ROCOP of PA and CHO using **2** as initiator and CHO as solvent and reagent [PA]$_0$:[CHO]$_0$:[**2**]$_0$ = 100:500:1, 80 °C (Table 2, entry 4). M_n^{GPC} and $Đ$ are calculated from GPC in THF using triple detection methods.

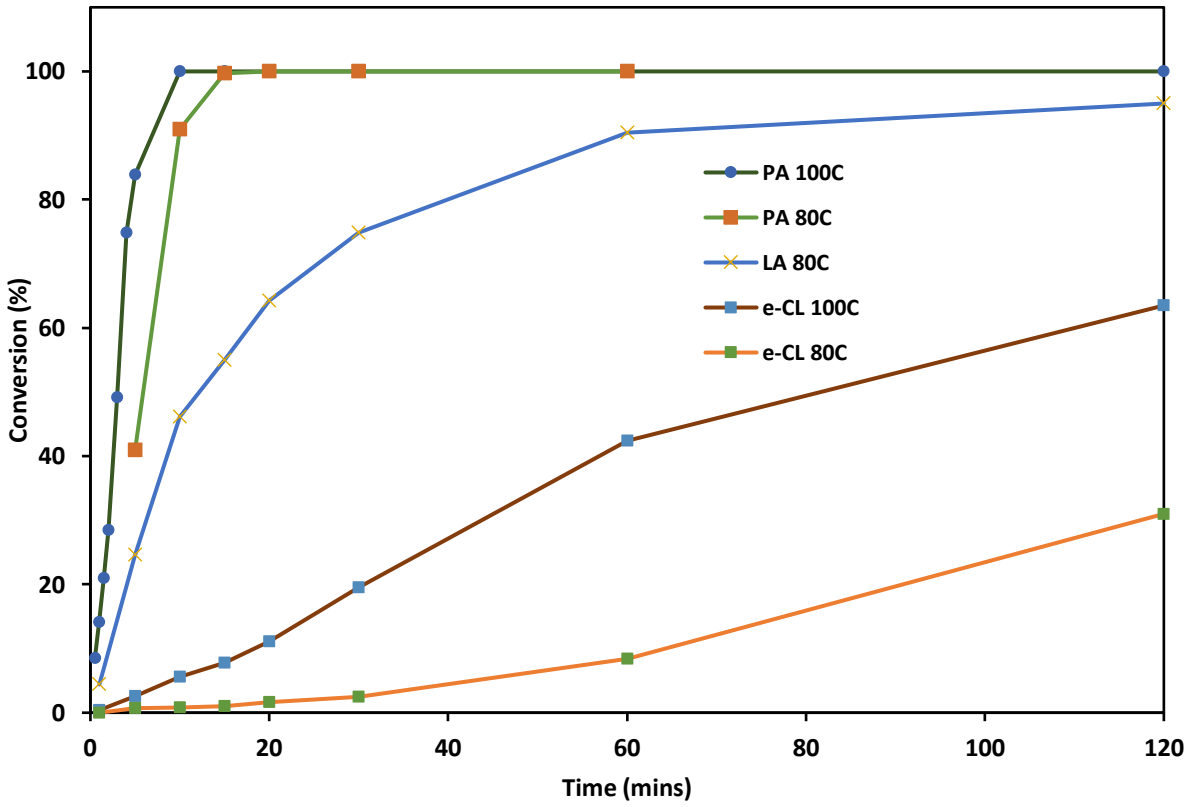

Figure S16. Conversion vs time plots for ROP of ε-CL and *rac*-LA, and ROCOP of PA and CHO using **2,** [M]$_0$:[CHO]$_0$:[**2**]$_0$ = 100:500:1, 80 °C or 100 °C as indicated.

^{1}H NMR for the synthesis of PCHC in the presence of ε-CL

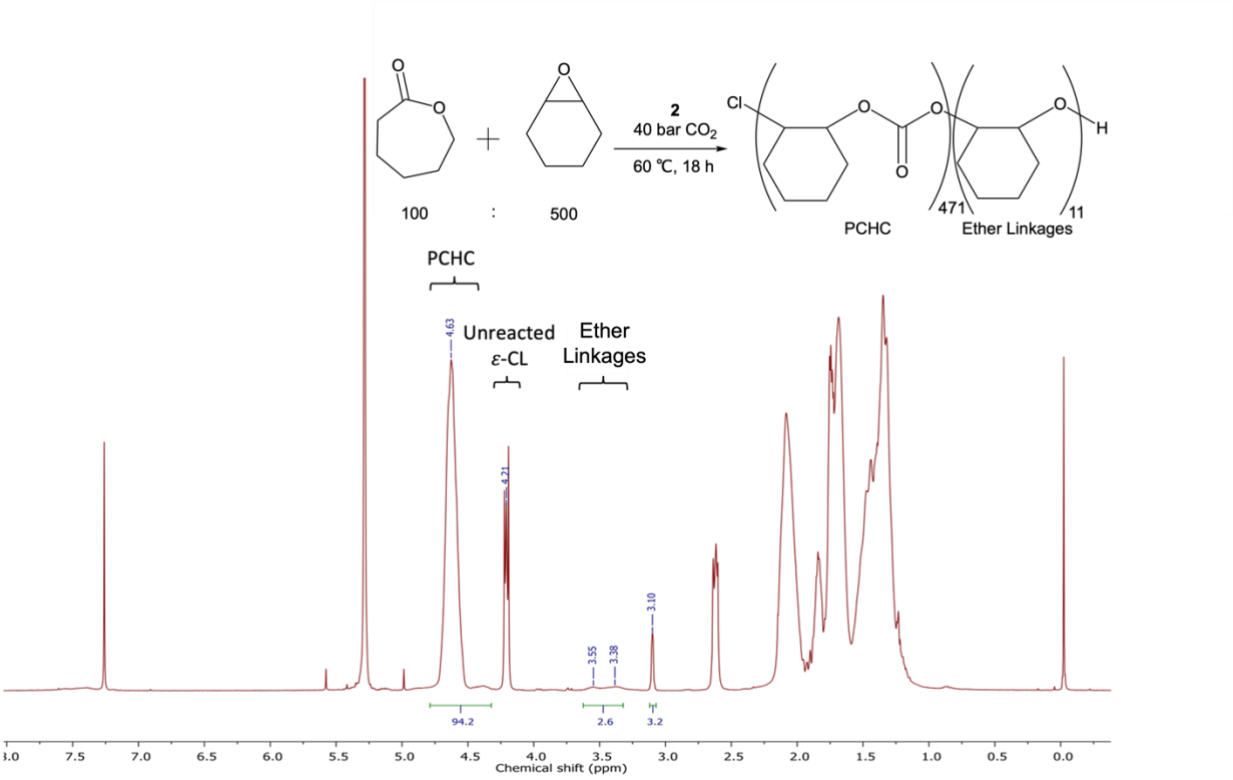

Figure S17. Crude ^{1}H NMR (300 MHz, $CDCl_3$) spectrum of the reaction of CHO and CO_2 in ε-CL $[\varepsilon\text{-CL}]_0$:$[CHO]_0$:[**2**]$_0$ = 100:500:1, 60 °C, 18h, 40 bar CO_2 (Table 3, entry 2).

^{1}H NMR and FTIR spectra of sequential CO_2 addition reactions

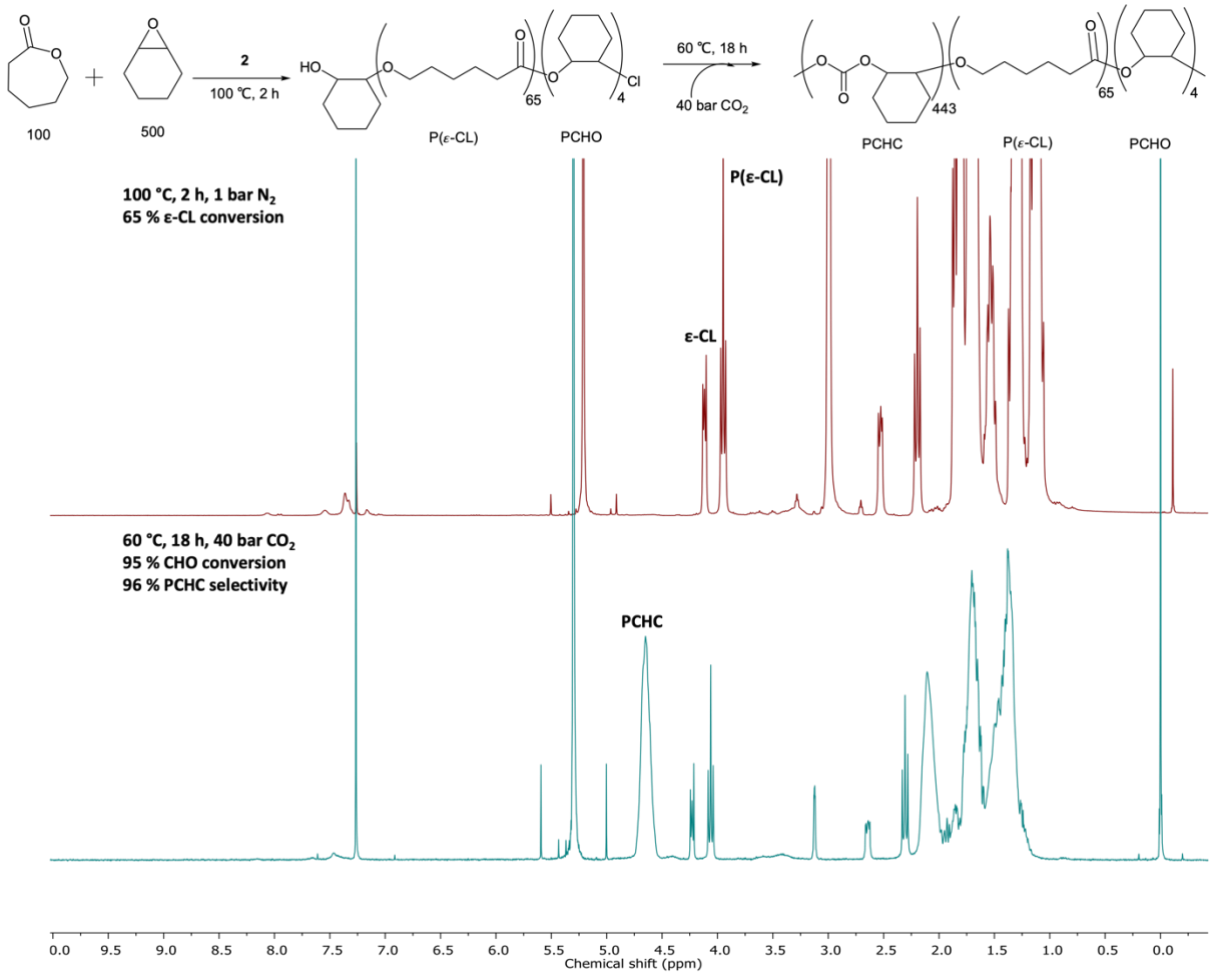

Figure S18. Stacked ^{1}H NMR (300 MHz, $CDCl_3$) spectra of the ROP of ε-CL in CHO using **2** as initiator, $[\varepsilon\text{-CL}]_0$:$[CHO]_0$:$[\mathbf{2}]_0$ = 100:500:1, 100 °C, 2 h followed by the sequential addition of 40 bar CO_2 to the polymer mixture and stirring at 60 °C for a further 22 h (Table 3, Entry 1). No further conversion of ε-CL is seen during the second sequence with no increase in polyether resonances.

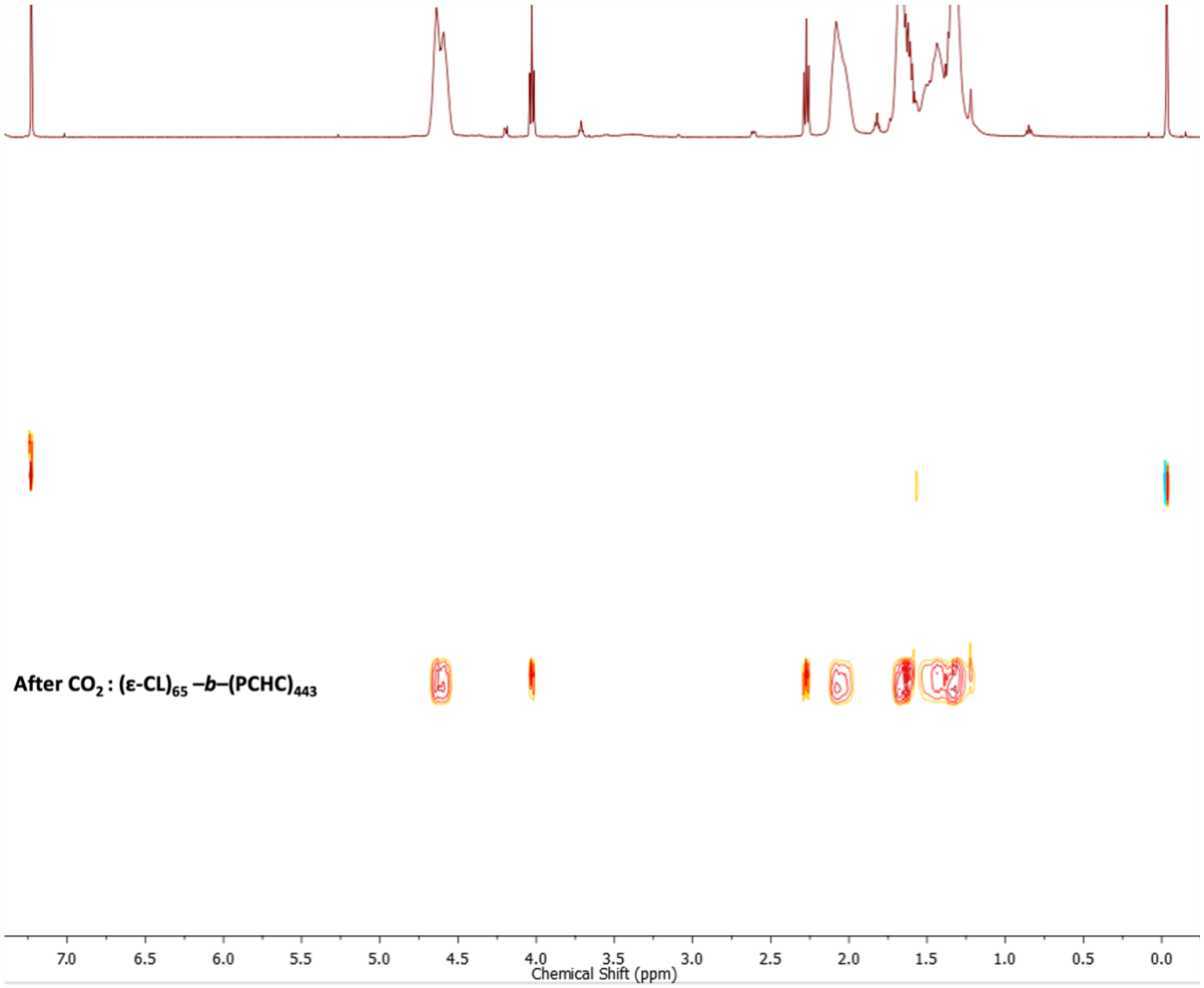

Figure S19. ^{1}H DOSY NMR (500 MHz, $CDCl_3$) spectrum of purified poly(ε-CL)$_{65}$ –*b*–PCHC$_{443}$ (Table 3, entry 1) confirming the presence of a block polymer and not individual poly(ε-CL) and PCHC polymers. Repeating unit ratios are estimated from crude ^{1}H NMR conversions.

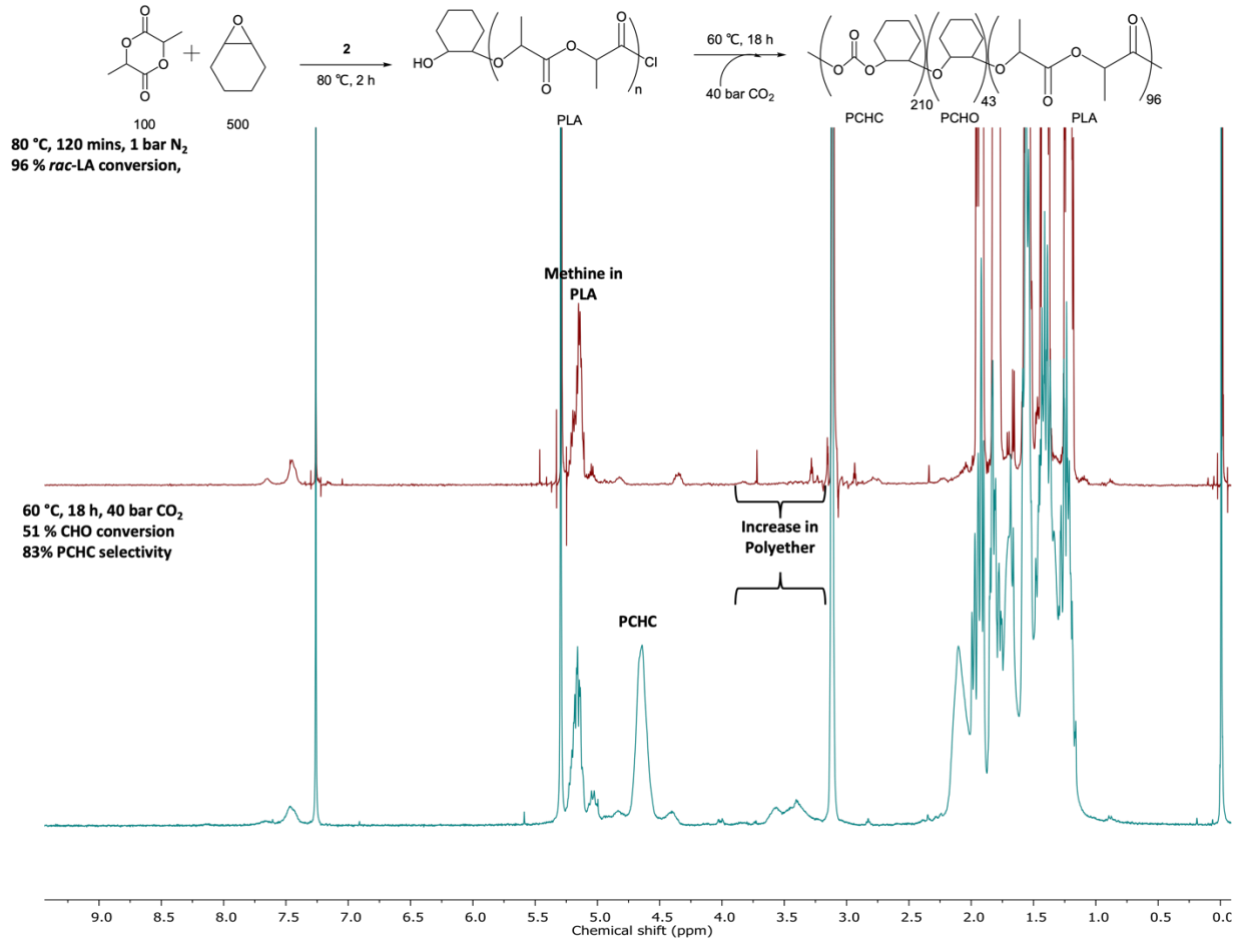

Figure S20. Stacked ^{1}H NMR (300 MHz, $CDCl_3$) spectra of the ROP of *rac*-LA in CHO using **2** as initiator, $[LA]_0$:$[CHO]_0$:$[\mathbf{2}]_0$ = 100:500:1, 80 °C, 2 h followed by the sequential addition of 40 bar CO_2 to the polymer mixture and stirring at 60 °C for a further 18 h (Table 3, entry 3). The presence of CHO polyether resonances (3.5 – 3.7 ppm) after CO_2 addition suggests the transesterification of polymer units.

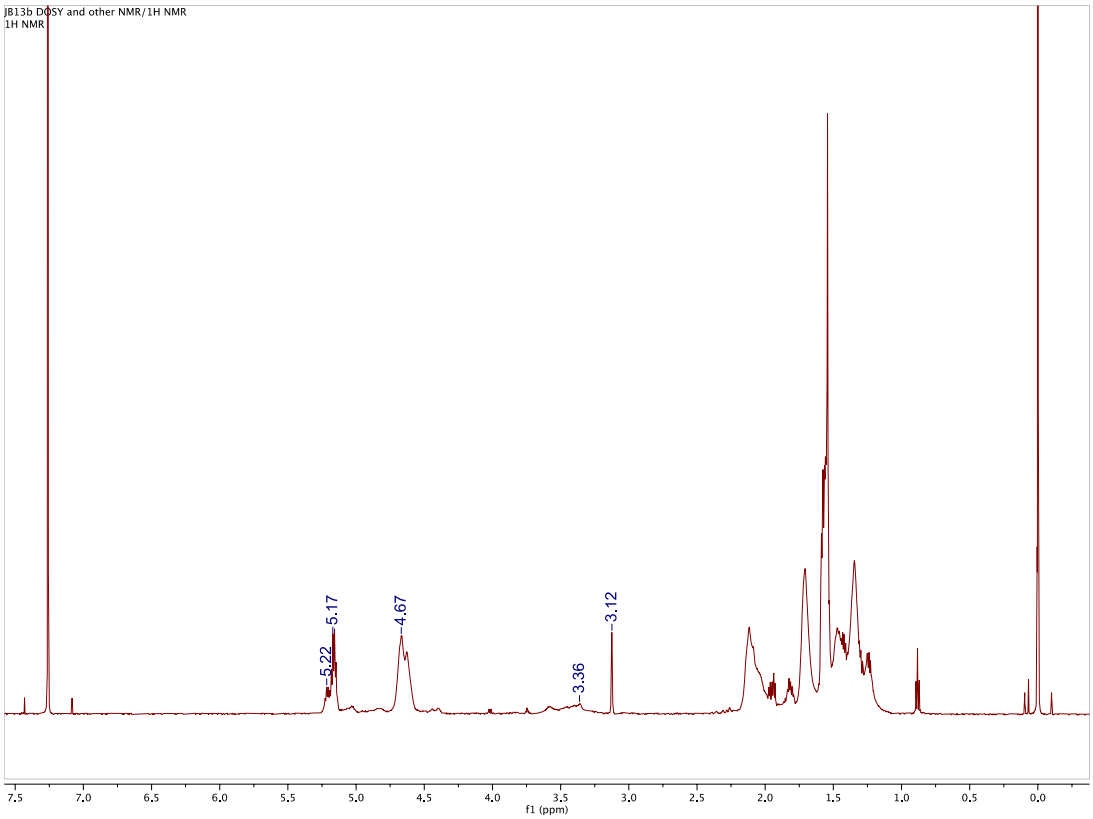

Figure S21. ^{1}H NMR (600 MHz, $CDCl_3$) spectrum of purified PLA_{96}-*b*-$PCHC_{210}$ (Table 3, entry 3). Repeating unit ratios calculated from crude ^{1}H NMR conversions from Figure S20.

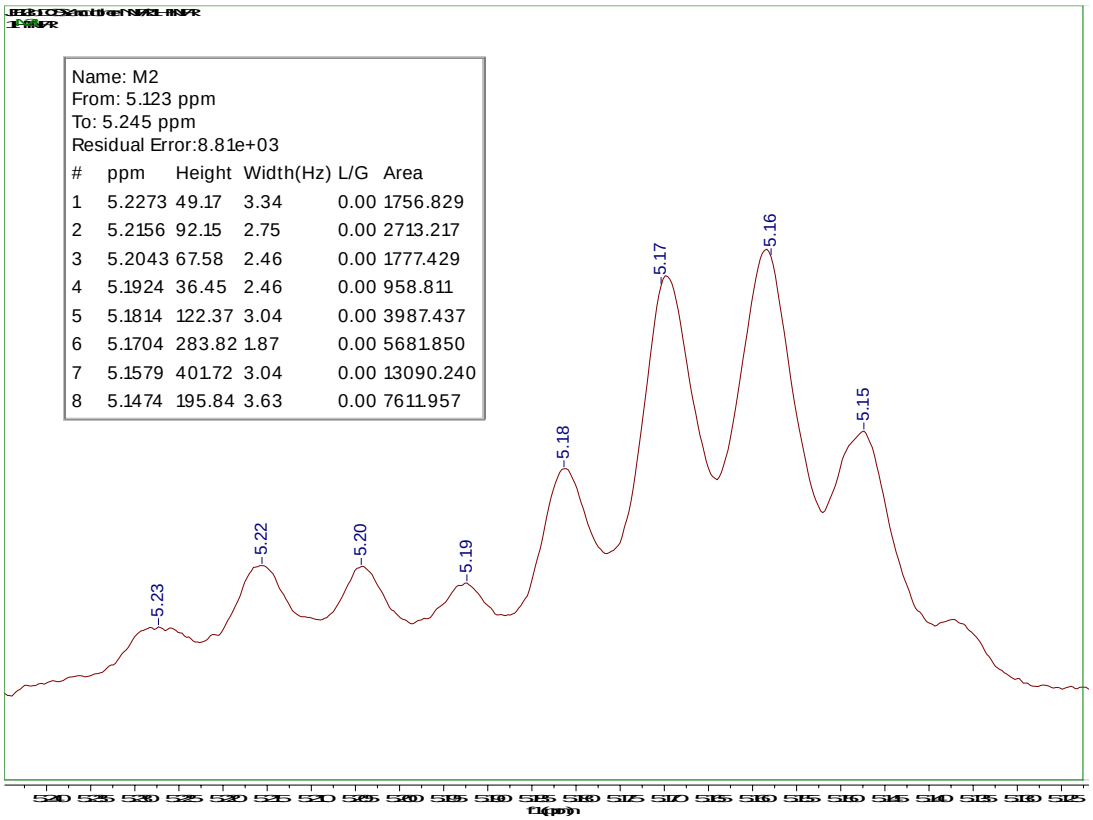

Figure S22. Expansion of the above ^{1}H NMR (600 MHz, $CDCl_3$) spectrum of purified PLA_{96}-*b*-$PCHC_{210}$ (Table 3, entry 3) in the 5.12 – 5.24 region of the spectrum for tacticity of PLA determination in the terpolymer. $P_r = 2I_1/(I_1 + I_2)$, with I_1 = 5.1875 – 5.24 ppm (rmr, mmr/rmm), I_2 = 5.13 – 5.1875 ppm (mmr/rmm, mmm, mrm).

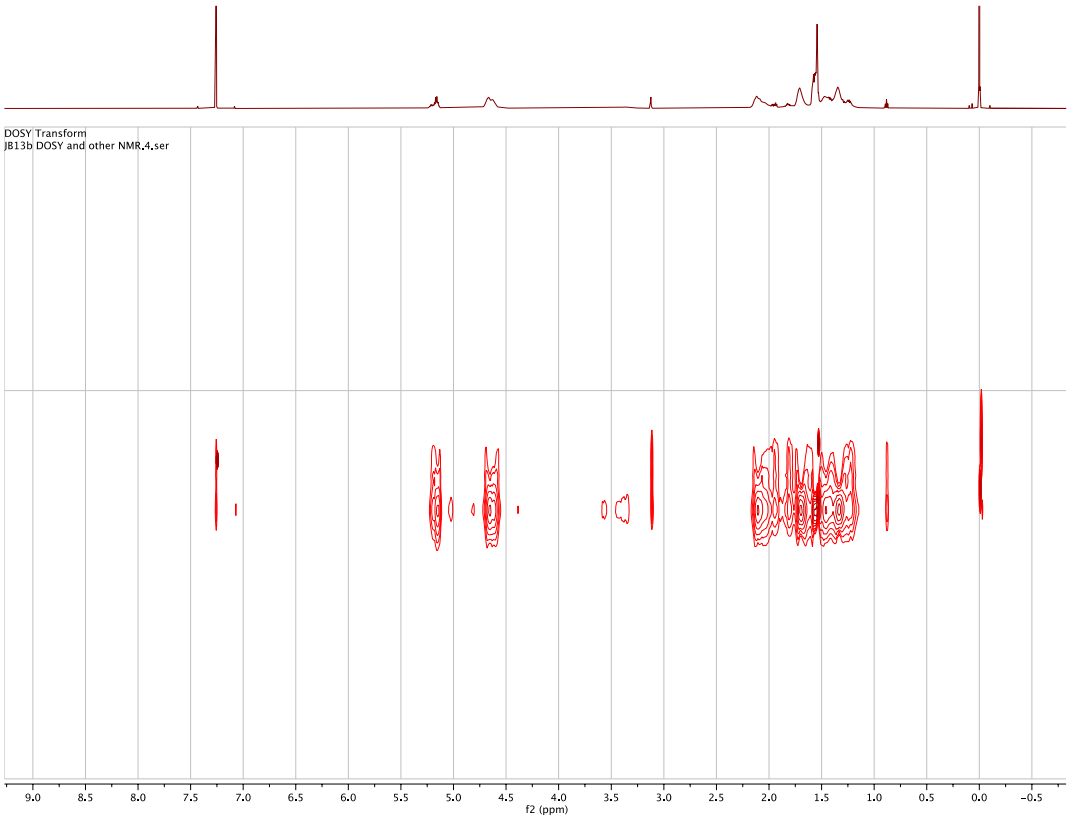

Figure S23. ^{1}H DOSY NMR (600 MHz, $CDCl_3$) spectrum of purified PLA_{96} –*b*–$PCHC_{210}$ confirming the formation of a single block polymer and not separate PLA and PCHC polymers for Table 3 entry 3. Repeating unit ratios are estimated from crude ^{1}H NMR conversions from Figure S20.

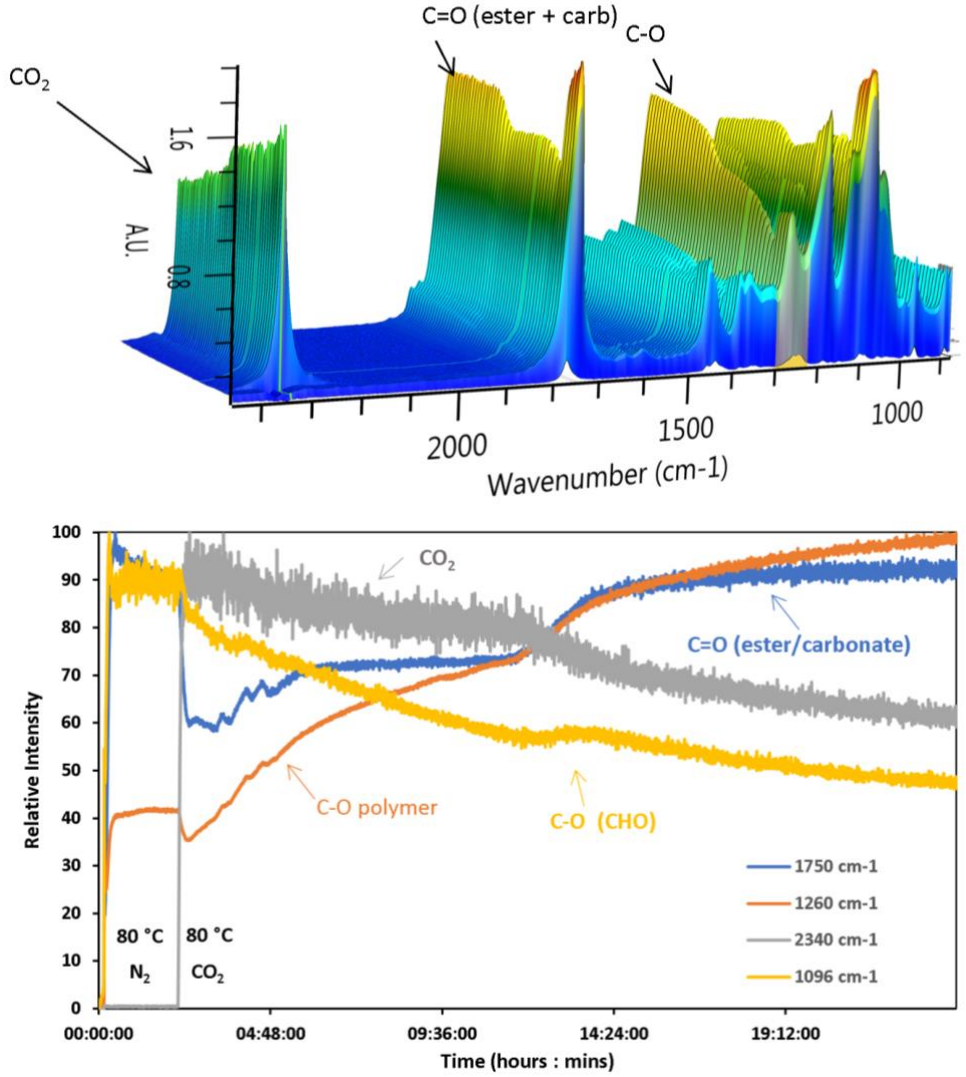

Figure S24. a) Stacked traces and b) plotted intensity of key bands from the *in-situ* FT-IR monitored ROP of *rac*-LA and sequential ROCOP of CHO and CO_2 at [*rac*-LA]$_0$:[CHO]$_0$:[**2**]$_0$ = 100:500:1. Sequence 1: 80 °C, 2 h, 1 bar N_2; Sequence 2) 80 °C, 22 h, 40 bar, CO_2 (Table 3, entry 4).

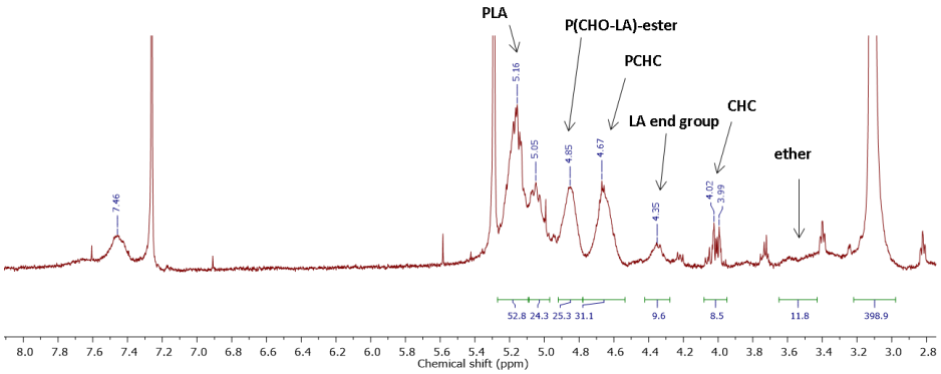

Figure S25. Crude ^{1}H NMR (300 MHz, $CDCl_3$) spectra from the *in-situ* FTIR monitored ROP of *rac*-LA and sequential ROCOP of CHO and CO_2 at [*rac*-LA]$_0$:[CHO]$_0$:[**2**] = 100:500:1. Sequence 1: 80 °C, 2 h, 1 bar N_2; Sequence 2) 80 °C, 22 h, 40 bar, CO_2 (Table 3, entry 4).

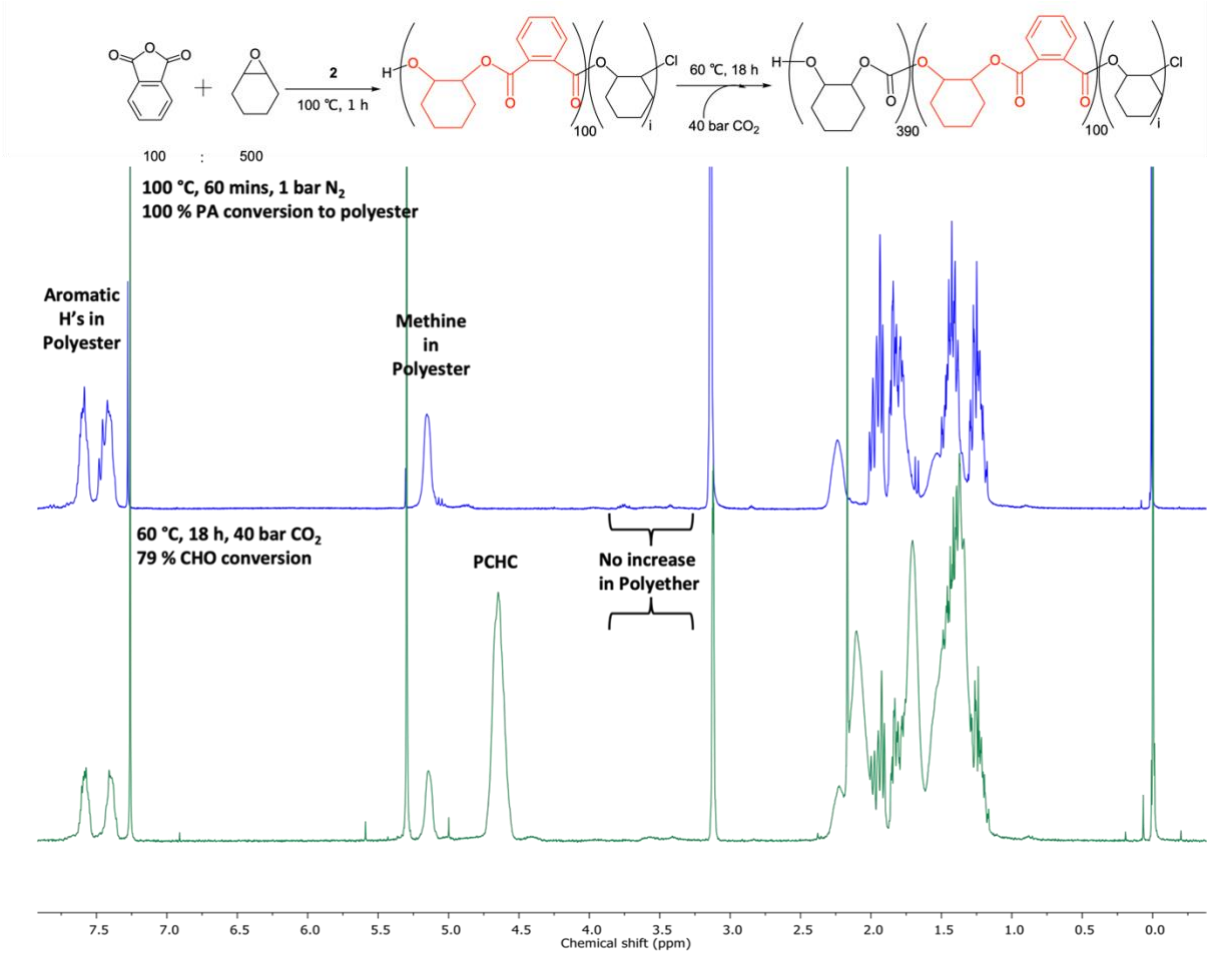

Figure S26. Stacked ^{1}H NMR (300 MHz, $CDCl_3$) spectra of the ROCOP of PA and CHO using **2** as initiator, $[PA]_0$:$[CHO]_0$:$[\mathbf{2}]_0$ = 100:500:1, 100 °C, 1 h, followed by the sequential addition of 40 bar CO_2 to the polymer mixture and stirring at 60 °C for a further 18 hours (Table 3, entry 5).

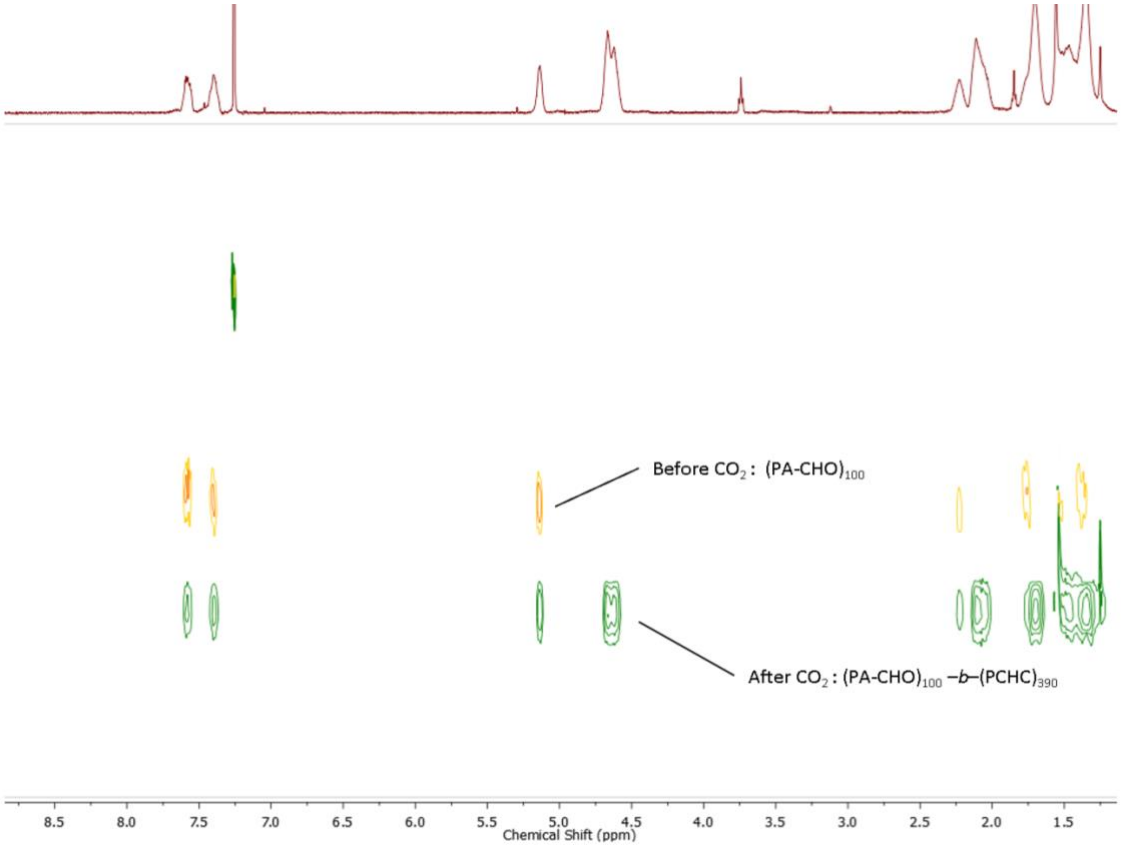

Figure S27. Stacked ^{1}H DOSY NMR (500 MHz, $CDCl_3$) spectra of purified polymers from the sequential reaction of CO_2 to a stirred solution of P(PA-*alt*-CHO)$_{100}$. Each sample shows D_{sol} =1.89 –1.91 x 10-9 $m^2\ s^{-1}$, repeating unit ratios are estimated from crude NMR conversions (Table 3, entry 5).

Selected gel permeation chromatography (GPC) traces

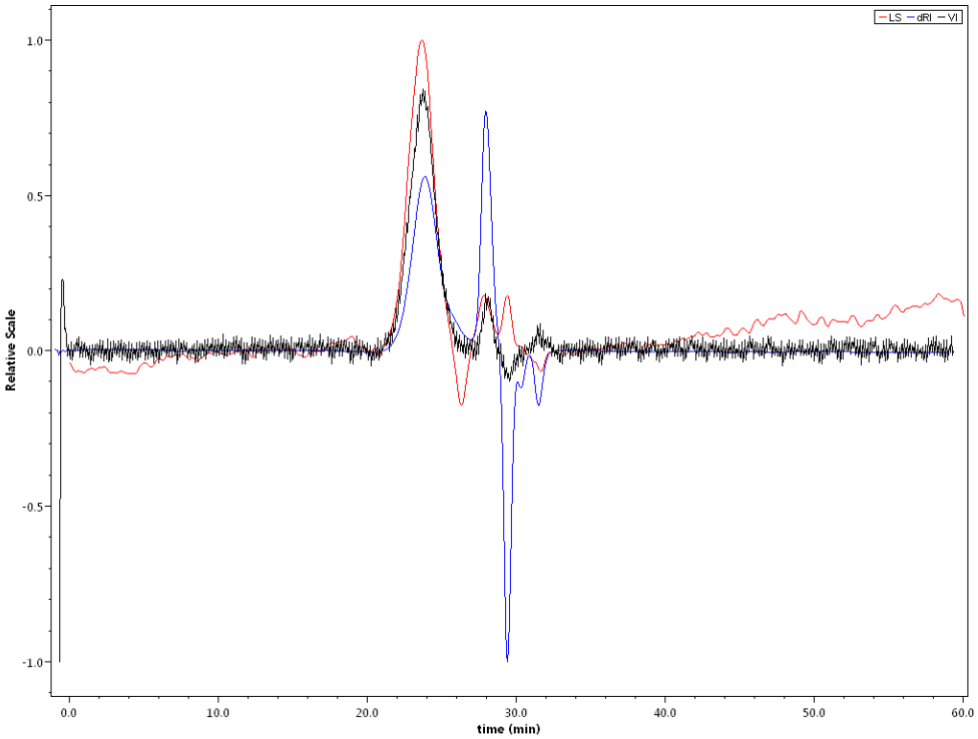

Figure S28. GPC trace for the ROP of *rac*-LA using **2** as initiator and CHO as solvent and co-initiator [*rac*-LA]$_0$:[CHO]$_0$:[**2**]$_0$ = 100:500:1, 80 °C, 2 h (Table 1, entry 8).

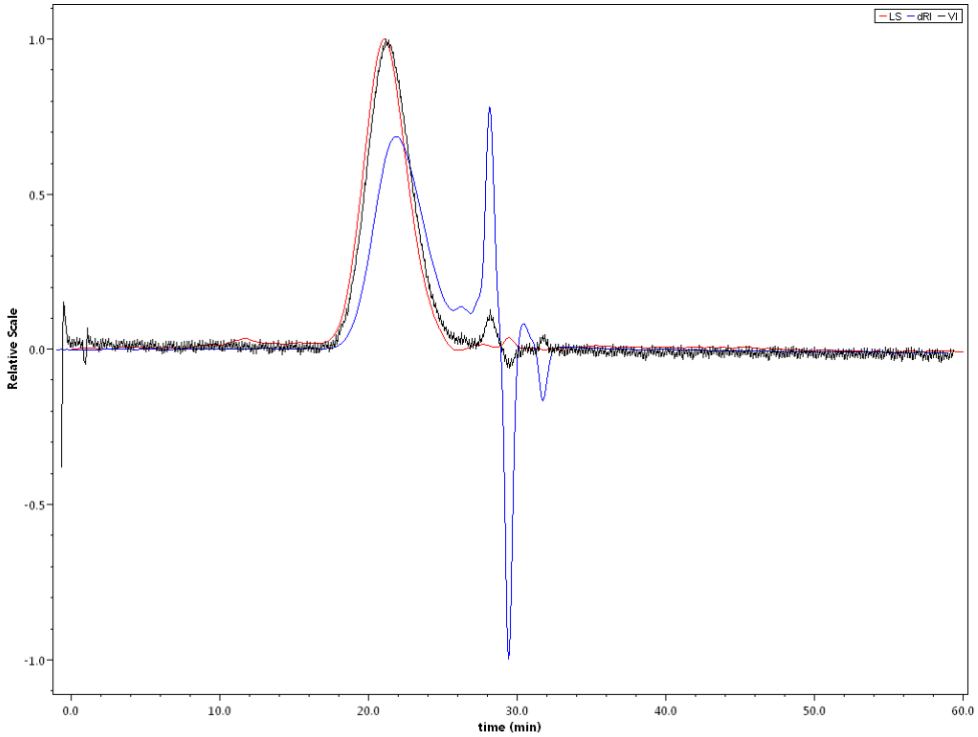

Figure S29. GPC trace for the ROP of ε-CL using **2** as initiator and CHO as solvent and co-initiator [ε-CL]$_0$:[CHO]$_0$:[**2**]$_0$ = 100:500:1, 100 °C, 2 h (Table 1, entry 12).

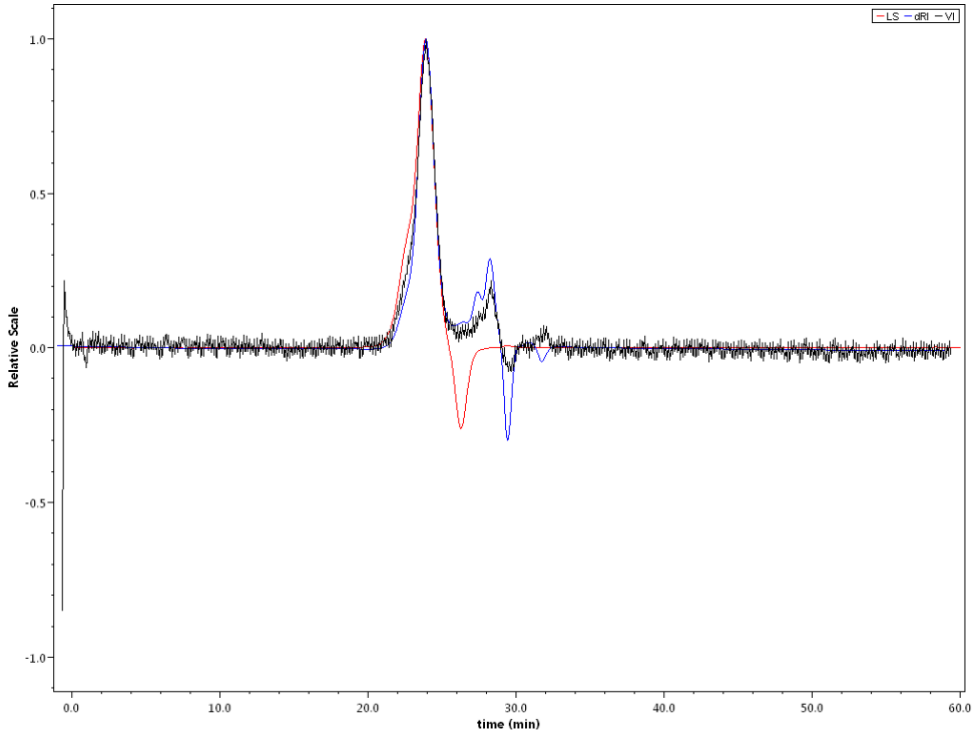

Figure S30. GPC trace for the ROCOP of PA using **2** as initiator and CHO as reactant and co-initiator $[PA]_0:[CHO]_0:[\mathbf{2}]_0$ = 100:800:1, 100 °C, 2 h (Table 2, entry 1).

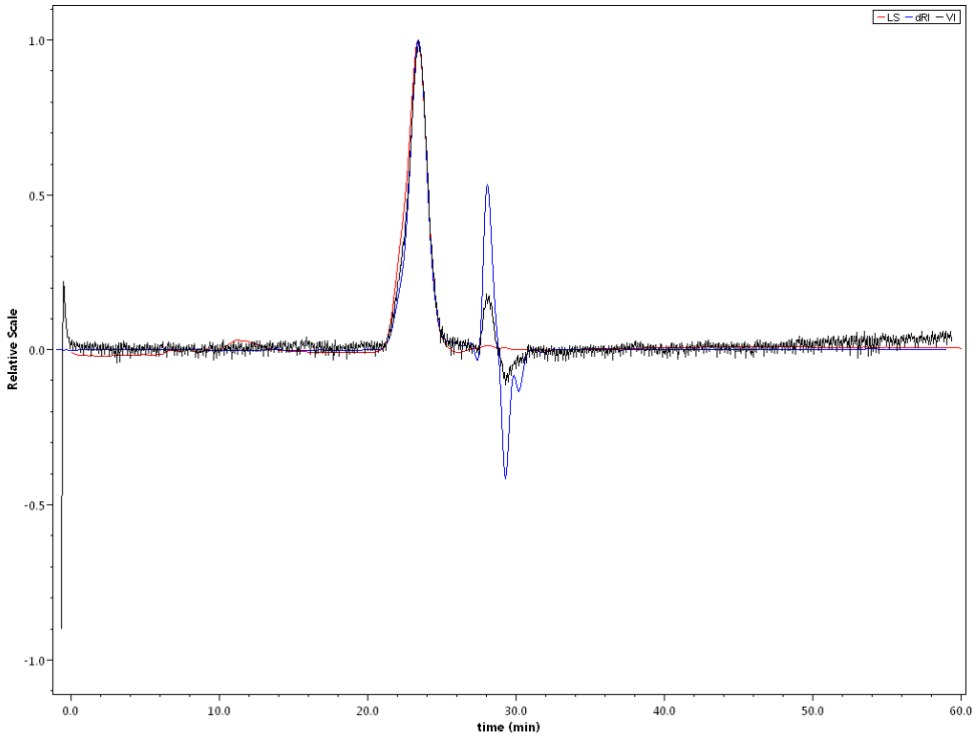

Figure S31. GPC trace for the ROCOP of PA using **2** as initiator and PO as reactant and co-initiator $[PA]_0:[PO]_0:[\mathbf{2}]_0$ = 100:500:1, 40 °C, 1.5 h (Table 2, entry 5).

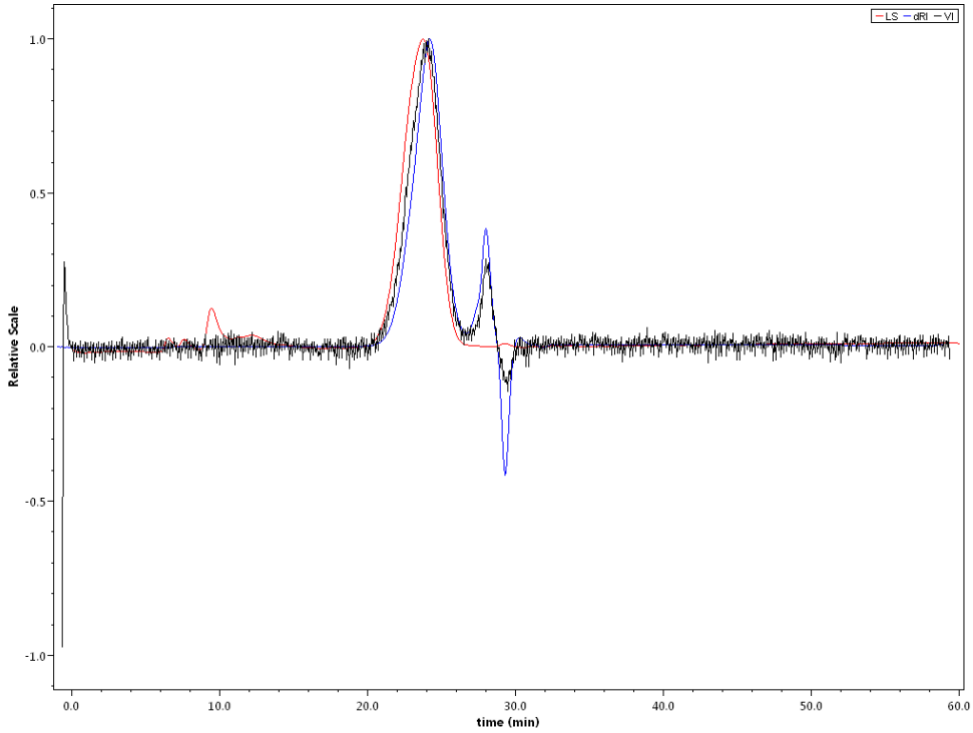

Figure S32. GPC trace for the ROCOP of PA using **2** as initiator and LO as reactant and co-initiator $[PA]_0:[LO]_0:[\mathbf{2}]_0$ = 100:500:1, 130 °C, 3 h (Table 2, entry 6).

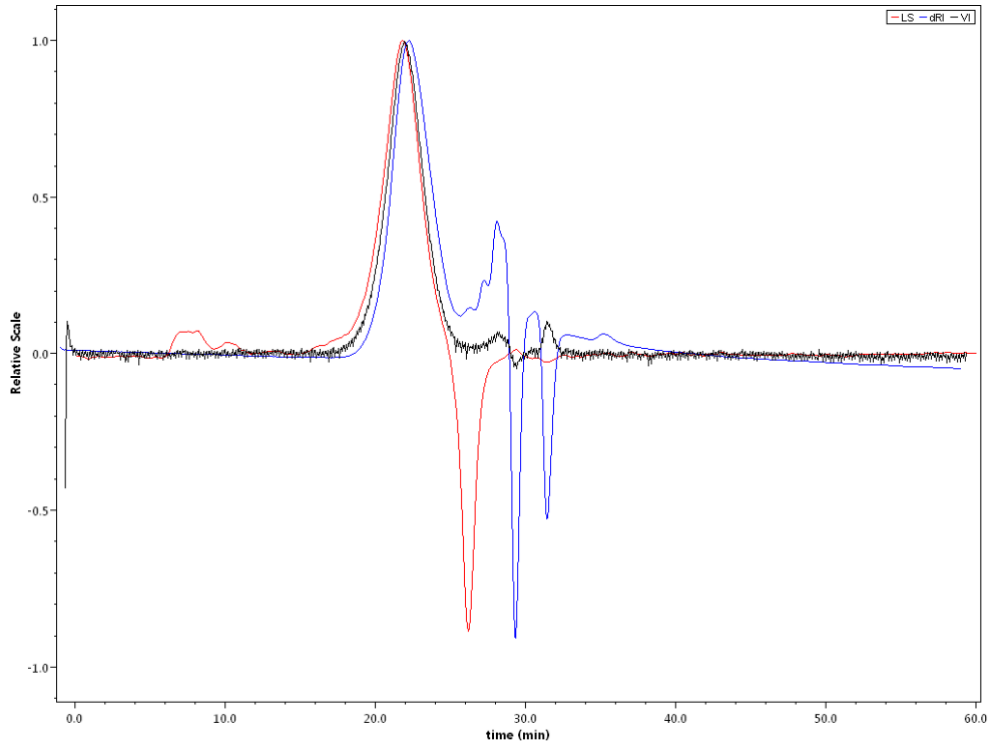

Figure S33. GPC trace for the ROCOP of PA using **2** as initiator and CHO as reactant and co-initiator prior to CO_2 addition $[PA]_0:[CHO]_0:[\mathbf{2}]_0$ = 100:500:1, 100 °C, 1 h (Table 3, entry 5).

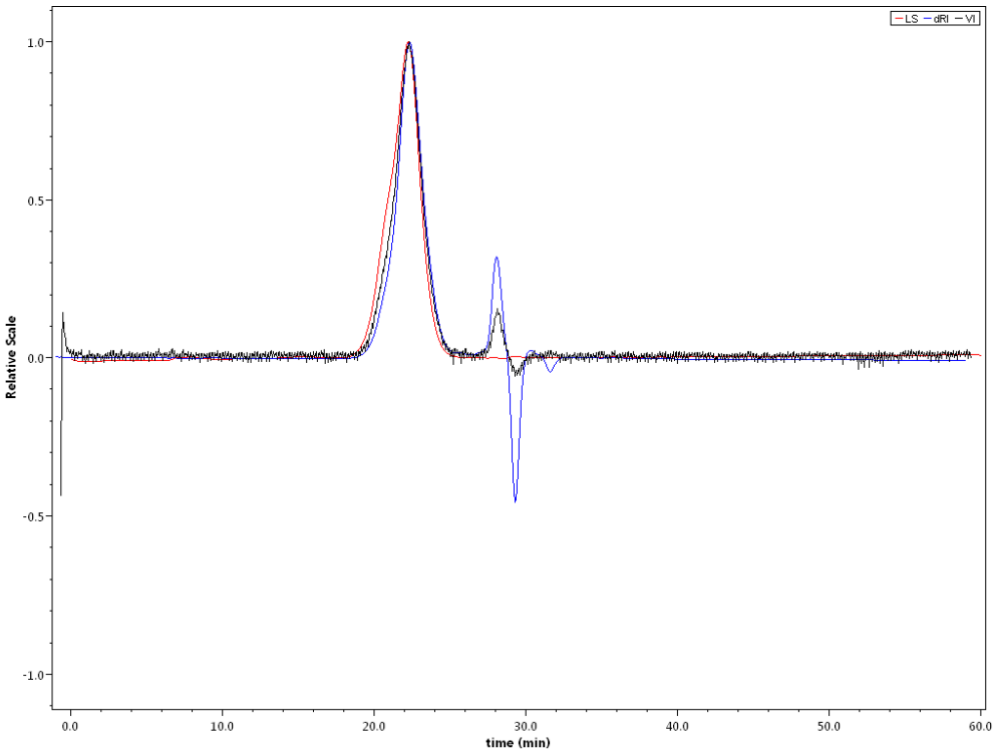

Figure S34. GPC trace for the ROCOP of PA using **2** as initiator and CHO as reactant and co-initiator after CO_2 addition $[PA]_0:[CHO]_0:[\mathbf{2}]_0$ = 100:500:1, 100 °C, 1 h, followed by 40 bar CO_2 at 60 °C for 18 h (Table 3, entry 5).

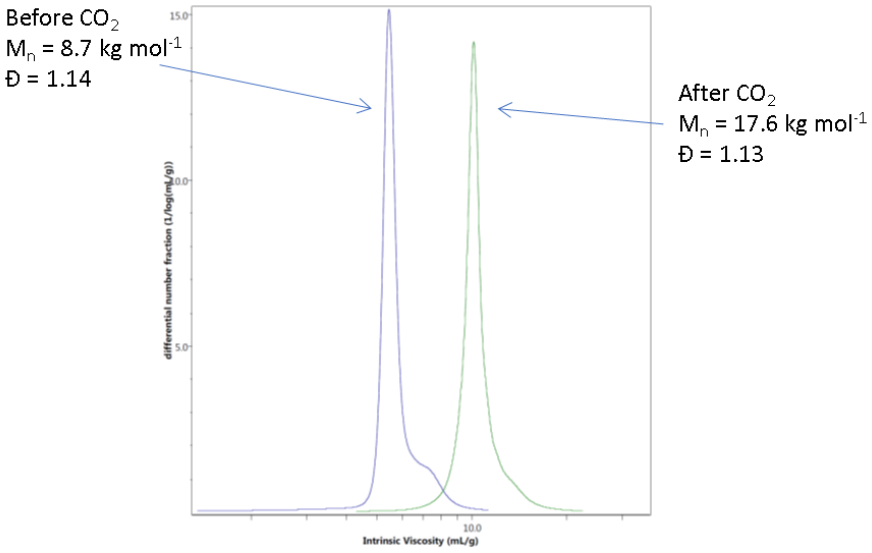

Figure S35. Differential number fraction vs intrinsic viscosity for the synthesis of polymers from the sequential reaction of CO_2 to a stirred solution of P(PA-*alt*-CHO)$_{100}$. (Table 3, entry 5)

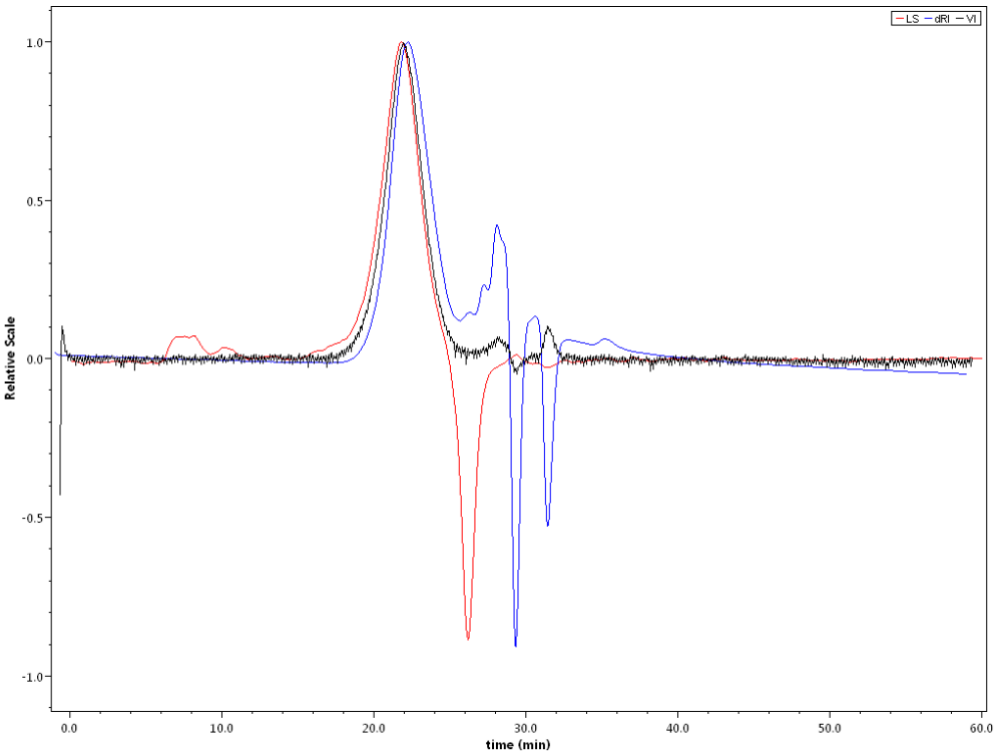

Figure S36. GPC trace for the ROP of ε-CL using **2** as initiator and CHO as solvent and co-initiator, **prior to CO_2 addition** $[\varepsilon\text{-CL}]_0:[\text{CHO}]_0:[\mathbf{2}]_0$ = 100:500:1, 100 °C, 2 h (Table 3, entry 1).

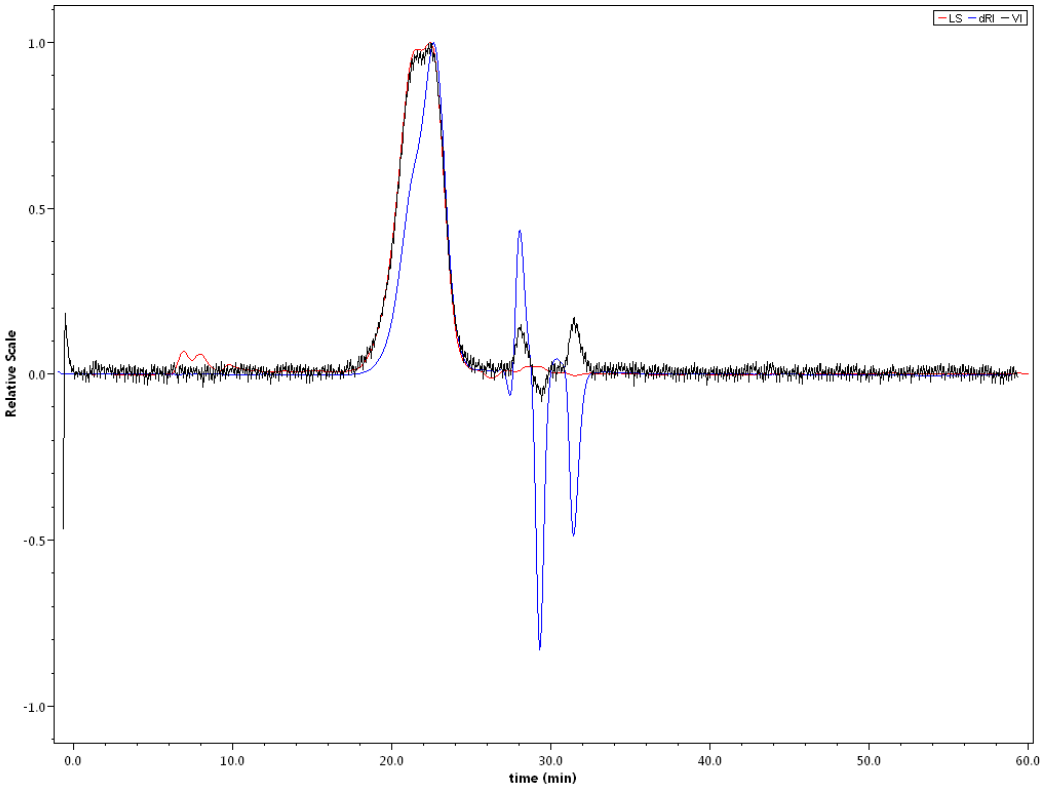

Figure S37. GPC trace for the ROP of ε-CL using **2** as initiator and CHO as solvent and co-initiator, **after CO_2 addition** $[\varepsilon\text{-CL}]_0:[\text{CHO}]_0:[\mathbf{2}]_0$ = 100:500:1, 100 °C, 2 h, followed by 40 bar CO_2 at 60 °C for 22 h (Table 3, entry 1).

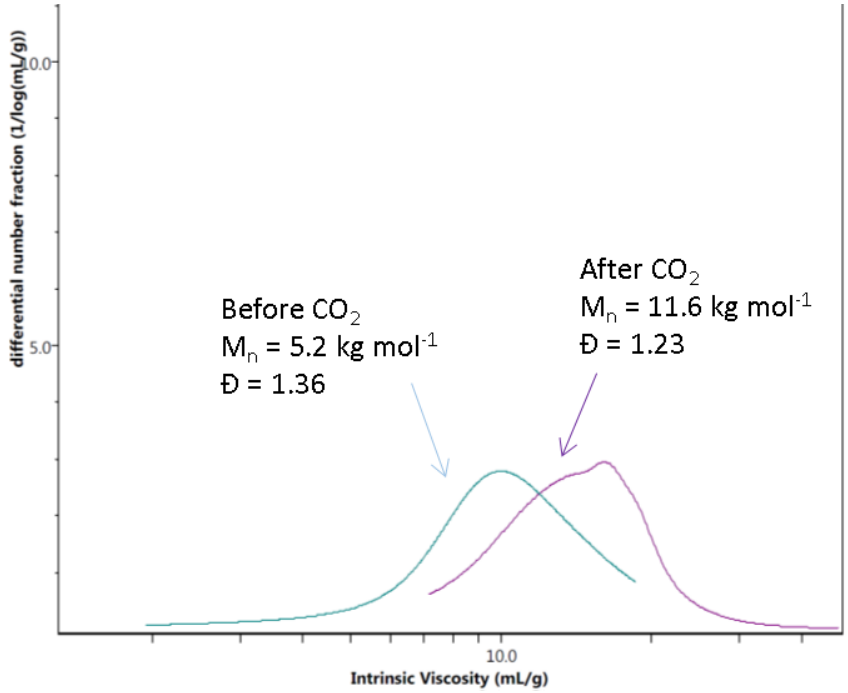

Figure S38. Differential number fraction vs intrinsic viscosity for the synthesis of polymers from the sequential reaction of CO_2 to a stirred solution of poly(ε-CL)$_{65}$. (Table 3, entry 1)

MALDI-TOF mass spectrometry of selected polymers

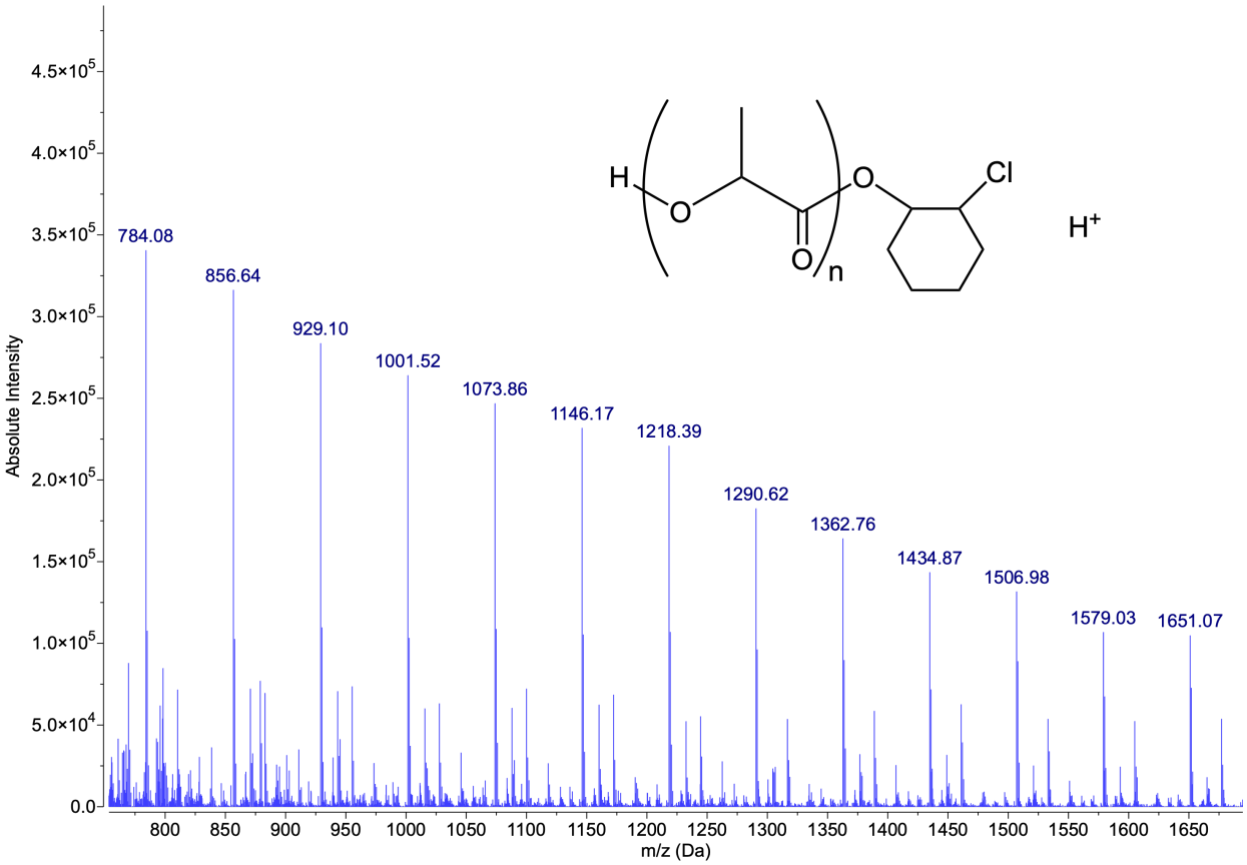

Figure S39. MALDI-TOF mass spectrum for the polymerization of *rac*-LA in CHO at 80 °C for 2 h using **2** (Table 1, Entry 8). Taken in positive reflectron mode.

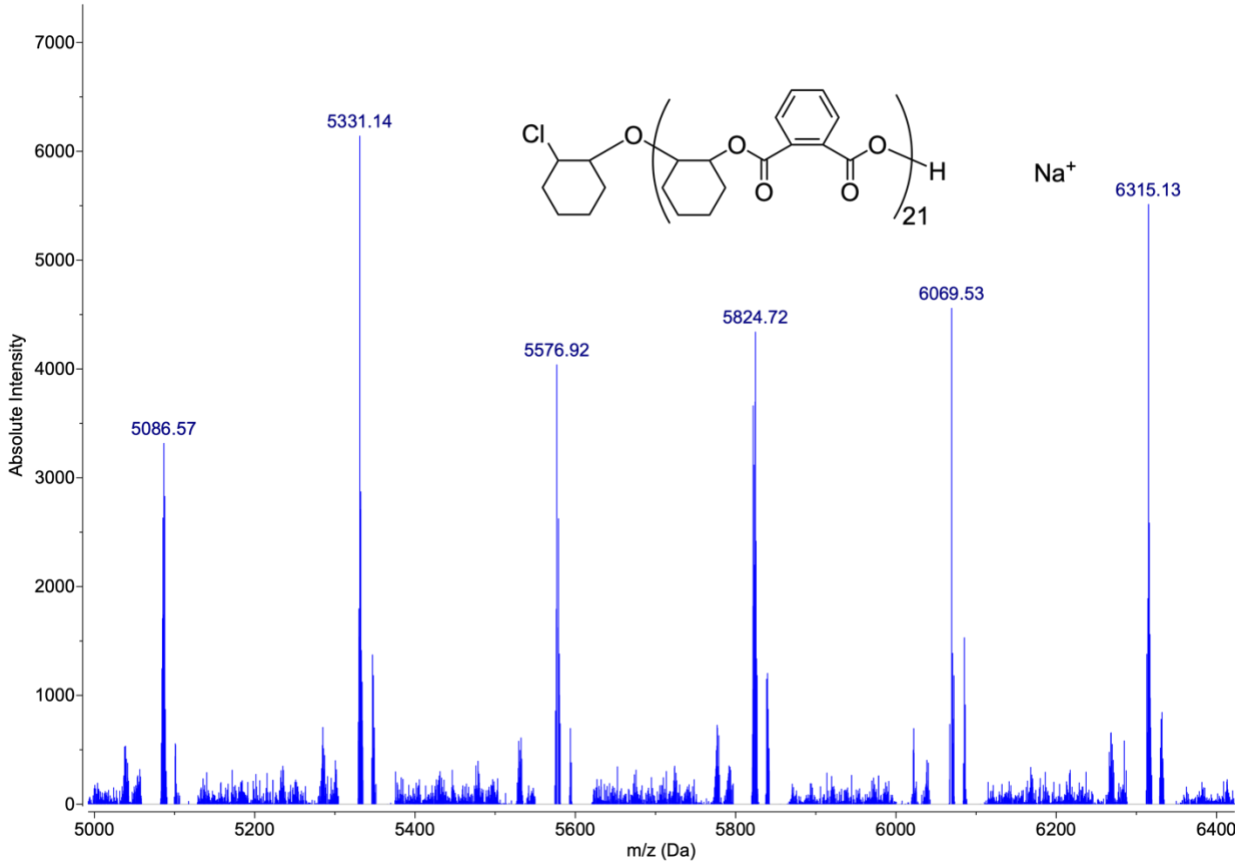

Figure S40. MALDI-TOF mass spectrum of the polyester produced containing CHO and PA at 100 °C for 1 h before CO_2 addition. (Table 3, entry 5 before CO_2 addition). Taken in positive reflectron mode.

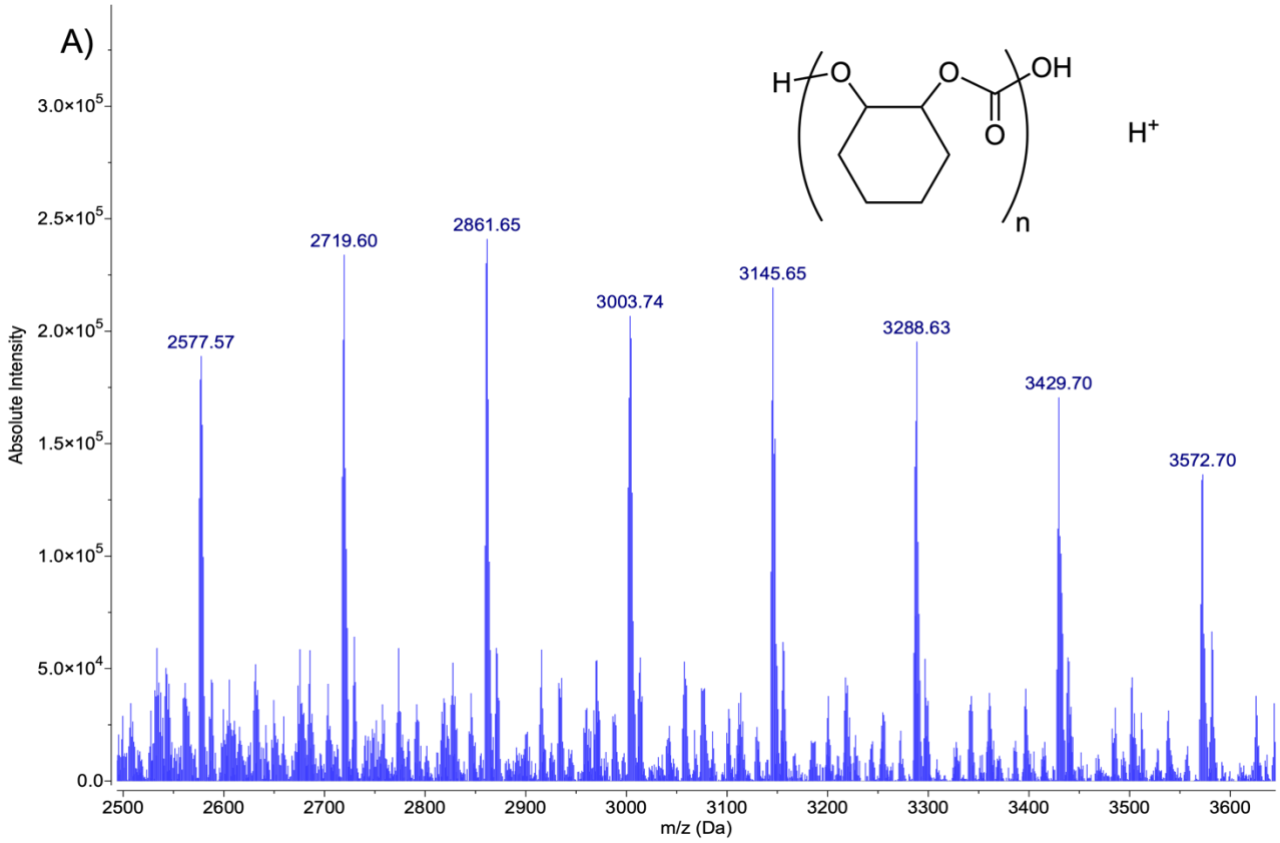
A)
Absolute Intensity
m/z (Da)
2577.57
2719.60
2861.65
3003.74
3145.65
3288.63
3429.70
3572.70
H
O
O
OH
O
n
H+

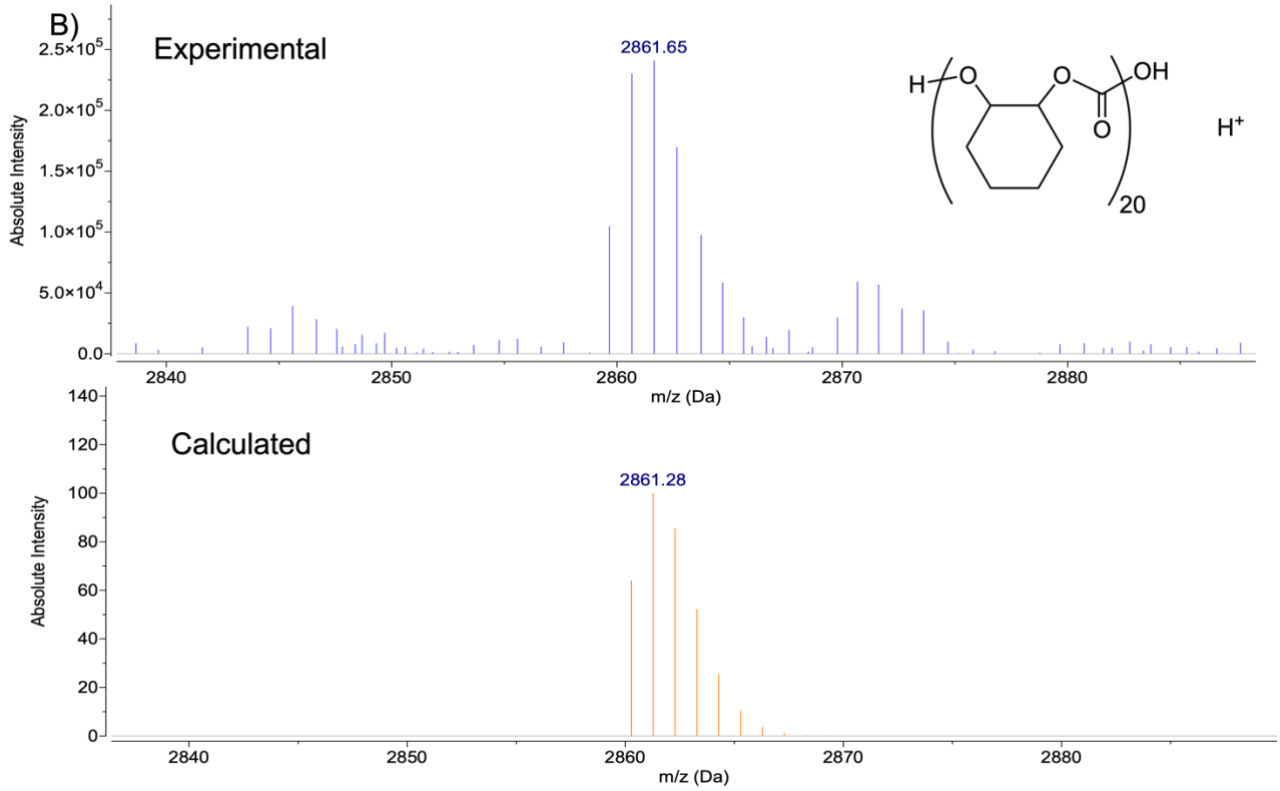
B)
Experimental
Absolute Intensity
m/z (Da)
2861.65
H
O
O
OH
O
20
H+
Calculated
2861.28

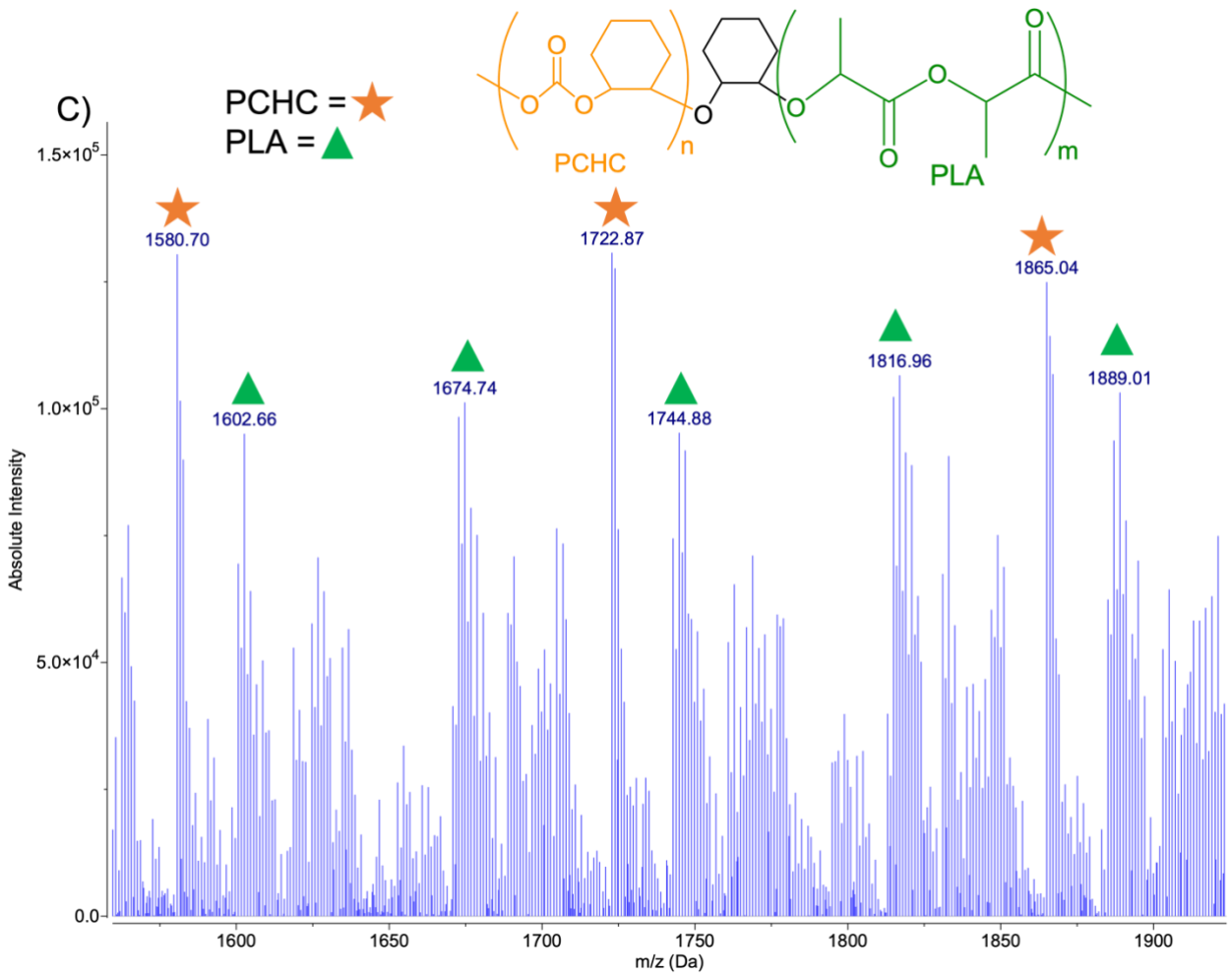

Figure S41. MALDI-TOF mass spectrum (positive reflectron mode) of the polymer produced from the reaction of *rac*-LA, CHO, and CO_2 at 80 °C for 2 h initially and 60 °C during CO_2 addition for 18 h according to conditions in Table 3, entry 3. A) and B) are from the higher *m/z* region which shows dominant cyclohexene carbonate repeating units, allowing end-group analysis. C) Shows lower *m/z* region with many overlapping peaks for both PLA and PCHC fragments of the terpolymer. End group analysis could not be readily performed for this region of the spectrum, and it is believed that the PLA ester to PCHC connection becomes broken under MALDI-TOF MS conditions causing the observed fragmentation in C).

Selected differential scanning calorimetry (DSC) thermograms

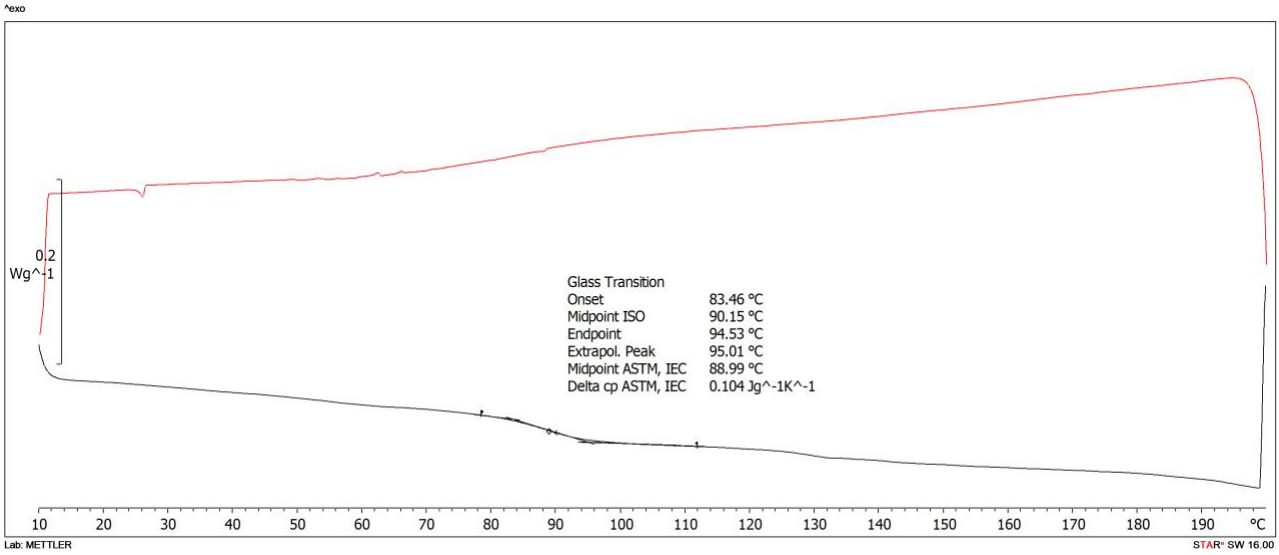

Figure S42. DSC thermogram for P(LO-*alt*-PA) polyester (Table 2, entry 7), 10 K min^{-1} heating rate under N_2 (50 mL min^{-1}). Second loop of heating and cooling used, red = cooling, black = heating, T_g obtained from the midpoint ISO for the given endotherm, T_g = 90 °C.

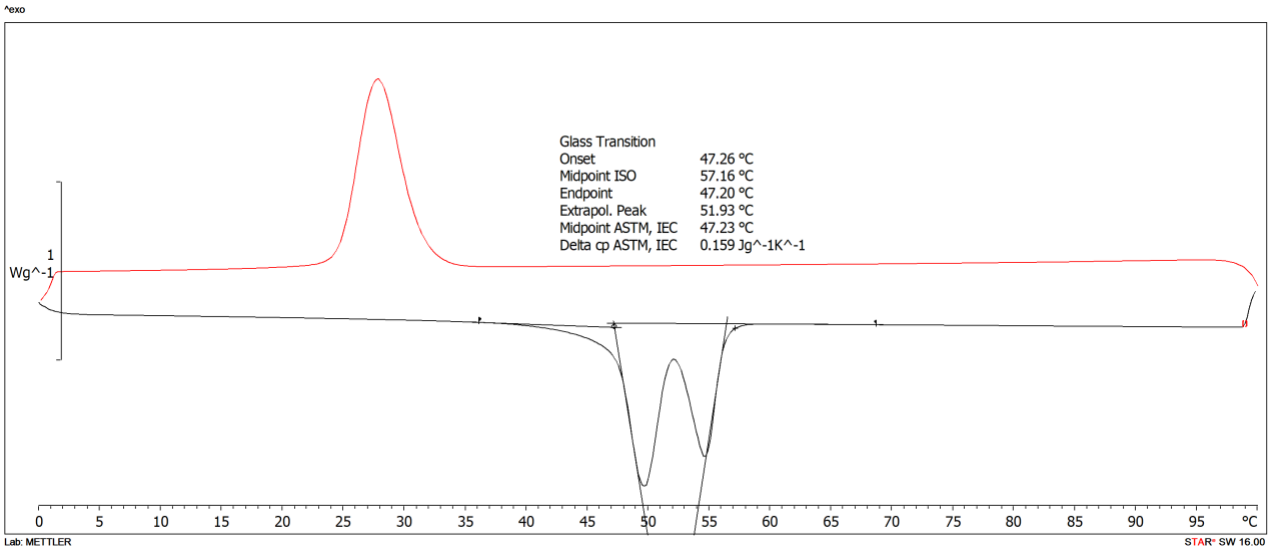

Figure S43. DSC thermogram for poly(ε-CL) (Table 3, entry 1 prior to CO_2 addition), 10 K min^{-1} heating rate under N_2 (50 mL min^{-1}). Second loop of heating and cooling used, red = cooling, black = heating, T_m obtained from the midpoint ISO for the given endotherm, T_m = 57 °C.

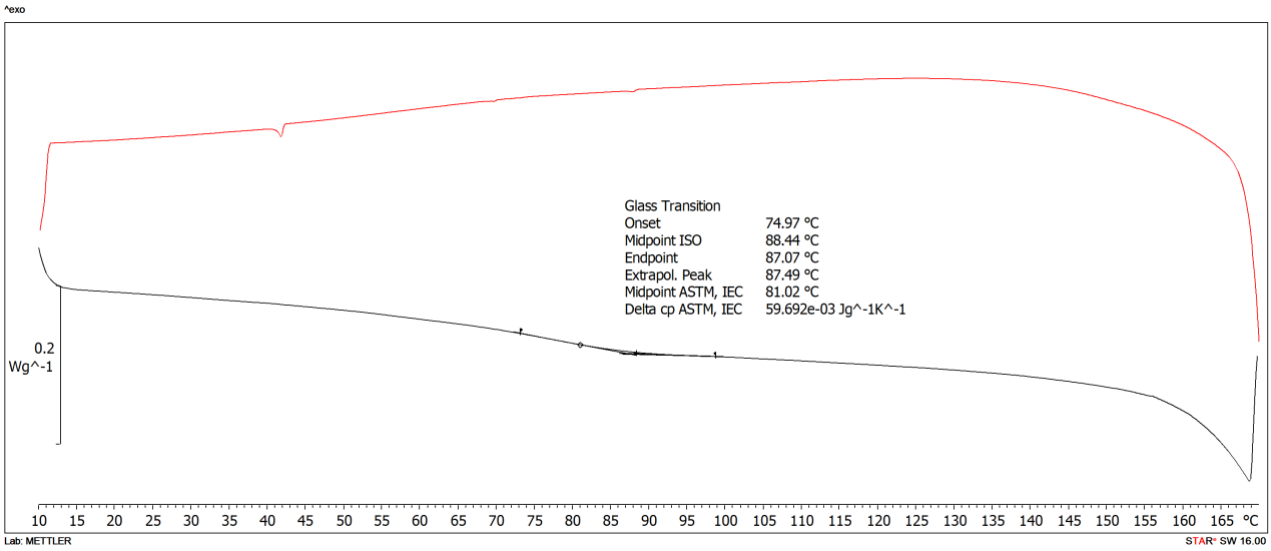

Figure S44. DSC thermogram for P(ε-CL)-*b*-PCHC (Table 3, entry 1 after CO_2 addition), 10 K min^{-1} heating rate under N_2 (50 mL min^{-1}). Second loop of heating and cooling used, red = cooling, black = heating, T_g obtained from the midpoint ISO for the given endotherm, T_g = 88 °C.

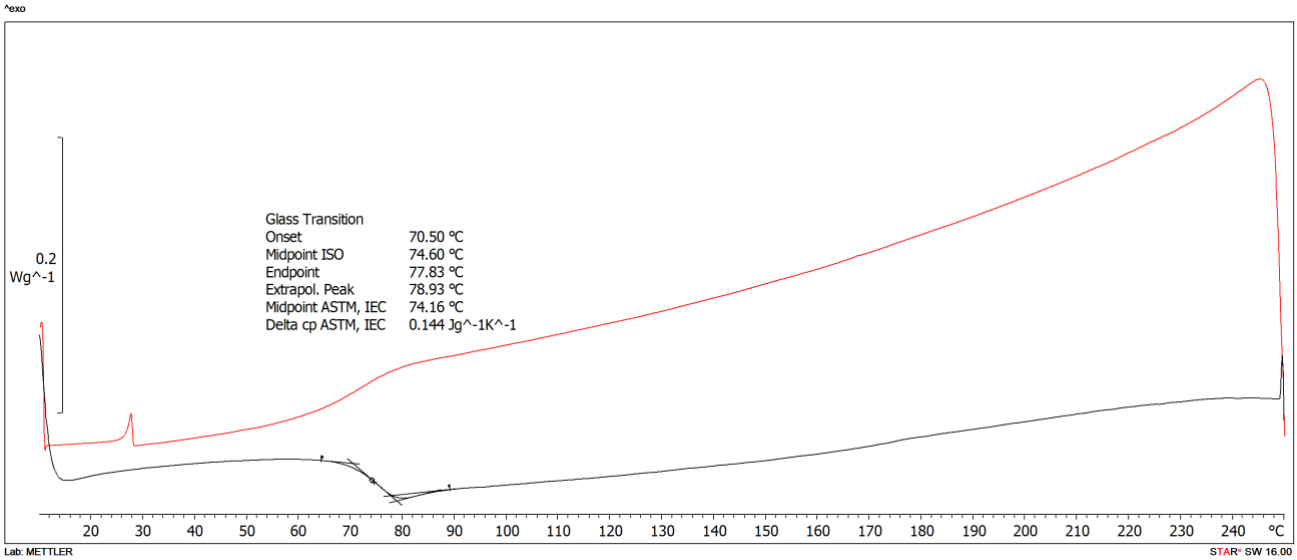

Figure S45. DSC thermogram PLA-*b*-PCHC (Table 3 entry 3 after CO_2 addition) 10 K min^{-1} heating rate under N_2 (50 mL min^{-1}). Second loop of heating and cooling used, red = cooling, black = heating, T_g obtained from the midpoint ISO for the given endotherm, T_g = 75 °C.

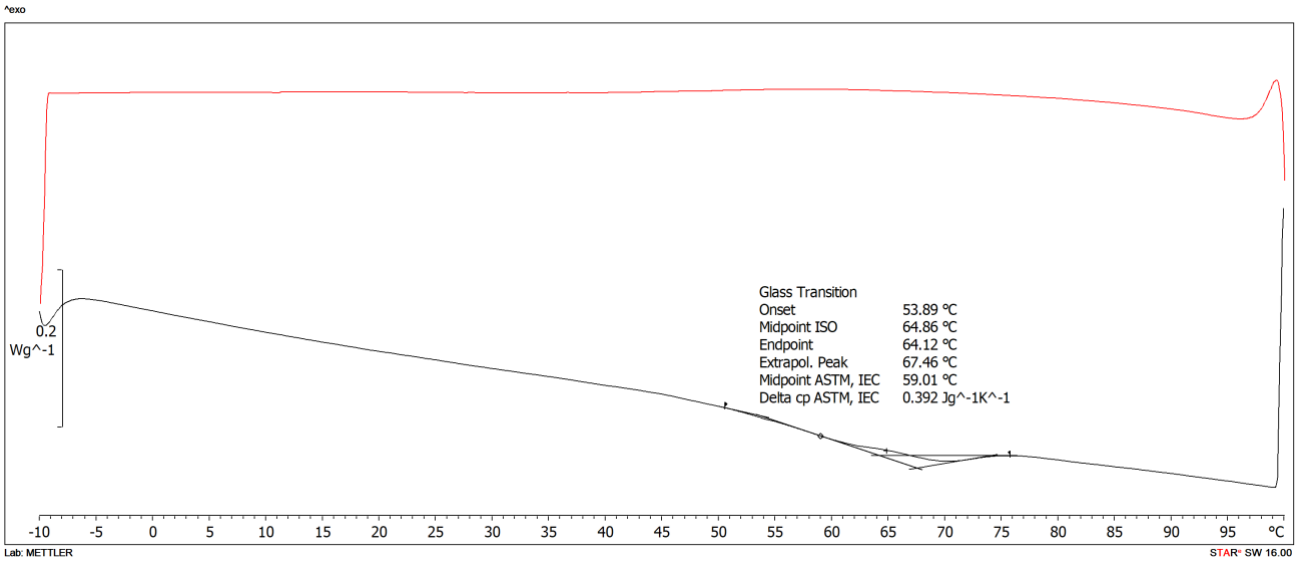

Figure S46. DSC thermogram PLA-*b*-PCHC (Table 3 entry 3 after CO_2 addition) 5 K min^{-1} heating rate under N_2 (50 mL min^{-1}). Second loop of heating and cooling used, red = cooling, black = heating, T_g obtained from the midpoint ISO for the given endotherm, T_g = 65 °C.

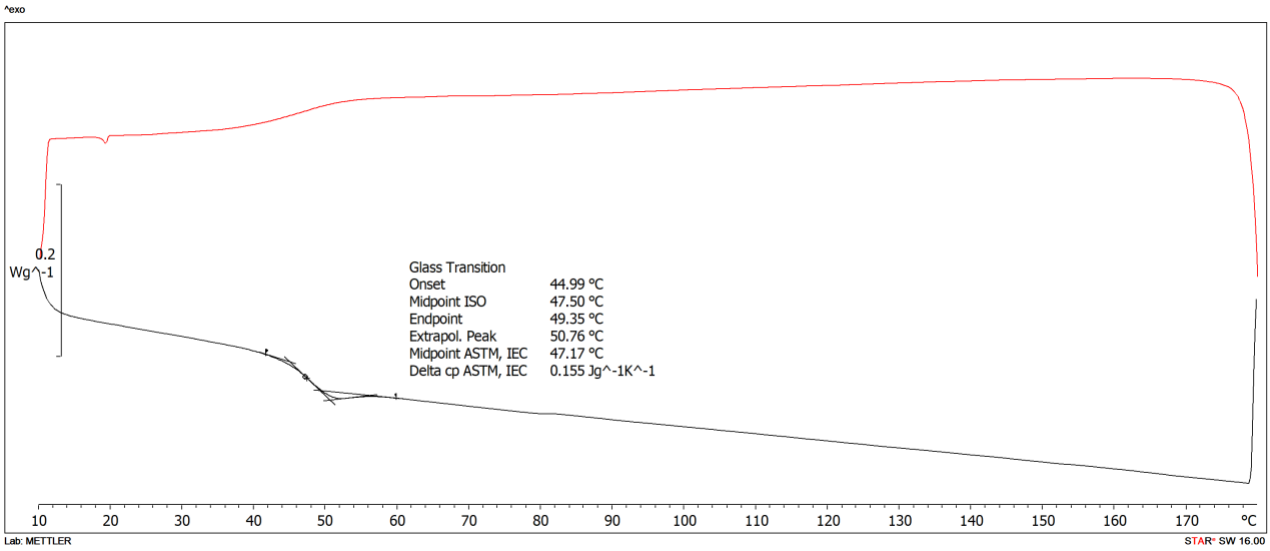

Figure S47. DSC thermogram for PLA-*b*-PCHC (Table 3, entry 4) after CO_2 addition. 10 K min^{-1} heating rate under N_2 (50 mL min^{-1}). Second loop of heating and cooling used, red = cooling, black = heating, T_g obtained from the midpoint ISO for the given endotherm, T_g = 48 °C.

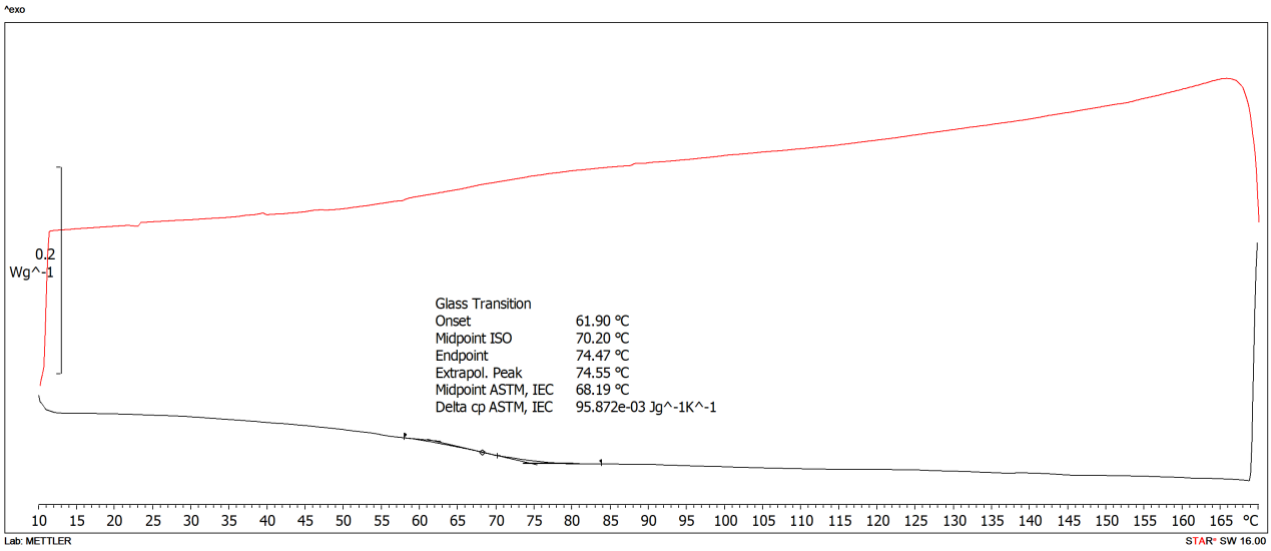

Figure S48. DSC thermogram for P(CHO-*alt*-PA) (Table 3, entry 5) before CO_2 addition. 10 K min^{-1} heating rate under N_2 (50 mL min^{-1}). Second loop of heating and cooling used, red = cooling, black = heating, T_g obtained from the midpoint ISO for the given endotherm, T_g = 70 °C.

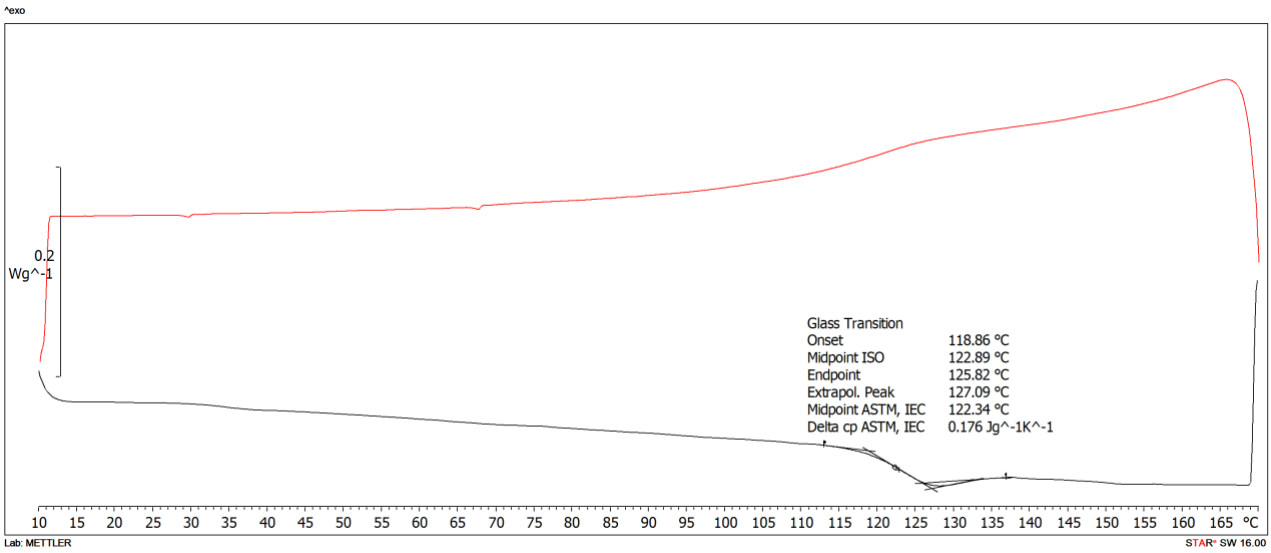

Figure S49. DSC thermogram for P(CHO-*alt*-PA)-*b*-PCHC (Table 3, entry 5) after CO_2 addition. 10 K min^{-1} heating rate under N_2 (50 mL min^{-1}). Second loop of heating and cooling used, red = cooling, black = heating, T_g obtained from the midpoint ISO for the given endotherm, T_g = 123 °C.